THEORETICAL AND EXPERIMENTAL ASPECTS OF PHOTOTRANSFERRED THERMOLUMINESCENCE FROM NATURAL AND SYNTHETIC QUARTZ

By

CHARLES SCOTT ALEXANDER

Bachelor of Science

University of California, San Diego

La Jolla, California

1994

Submitted to the Faculty of the
Graduate College of the
Oklahoma State University
in partial fulfillment of
the requirements for
the Degree of
MASTER OF SCIENCE
July, 1996

THEORETICAL AND EXPERIMENTAL

ASPECTS OF PHOTOTRANSFERRED

THERMOLUMINESCENCE FROM

NATURAL AND SYNTHETIC

QUARTZ

Thesis Approved:

Thesis Advisor

Dean of the Graduate College

ACKNOWLEDGMENTS

I wish to express my appreciation of those people who have helped in the preparation of this thesis. Primarily, I wish to thank my advisor, Dr. S.W.S. McKeever, whose helpful guidance and insight were invaluable. The helpful remarks of Dr. R. Chen on the topics of chapter II are gratefully acknowledged. I would also like to thank the other members of Dr. McKeever's research group for their help and support. In addition, I must thank the Department of Physics for their financial support during the past two years. I am also grateful for the love and support of my family. Finally, I extend my deepest appreciation to my wife, Wendy, for her support, encouragement, and love throughout this endeavor.

TABLE OF CONTENTS

Chapter Page

LIST OF TABLES

LIST OF FIGURES

Figure Page

Figure Page

Figure Page

CHAPTER I

INTRODUCTION

What is Thermoluminescence?

Thermoluminescence (TL) is the thermally stimulated emission of light from an insulator or semiconductor upon heating after the absorption of energy by irradiation. TL is distinguished from incandescence by the property that the energy released has been previously absorbed (e.g. from irradiation). Also, TL generally occurs at lower temperatures than incandescence and therefore is sometimes referred to as 'cold light'.

History of TL

TL has been known to man for many centuries. Medieval alchemists knew that some minerals glowed faintly when heated in the dark (Becker, 1973). The first scientifically documented observation of TL was made by Robert Boyle on October 28, 1663 (Boyle, 1663). In a paper read before the Royal Society, he reported in part, "I also brought [a diamond] to some kind of Glimmering Light, by taking into bed with me, and holding it a good while against a warm part of my Naked Body."

Since Boyle made his observation, physicists and chemists have studied TL However, since TL emissions are generally faint, the only practical use of TL was as a tool in mineral identification until the photomultiplier was available as a sensitive light detector

in the 1940s. In the 1950s the use of TL in dosimetry, the measurement of exposure to radiation, was initially developed at the University of Wisconsin (Daniels, Boyd, and Saunders, 1953). Here, the use of TL in archaeological and geological age determination was suggested. Following this suggestion, TL from ancient pottery was first detected at the University of Bern (Grögler, Houtermans, and Stauffer, 1960) and the University of California (Kennedy and Knopff, 1960). Immediately following these observations, processes using TL for archaeological dating were developed at several laboratories around the world. Methods of dating archaeological samples have continued to be developed and refined since that time. As of 1985, there were more than 40 labs researching TL for dating purposes. Methods for dating pottery have been extended to other applications, including determining the age of deposition of sediments and authenticity testing of art objects.

TL Dating

The natural TL (TL not induced by laboratory irradiation) from samples is induced by irradiation from natural radioactive sources present in the surrounding material (^{40}K, ^{232}Th, ^{238}U, ^{235}U, and ^{87}Ru and their daughter products) and by cosmic radiation (although this contribution is slight). Aitken (1985) gives a detailed discussion in chapter 4 of his book "Thermoluminescence Dating". These radiation sources are assumed to provide a nearly constant dose rate. This dose rate can be calculated taking into account the radioactive materials present and external effects such as disequilibrium, the loss of

gaseous radioactive daughter products, such as radon. The most basic of TL dating techniques is based on this assumption. Having determined the amount of TL present in a natural sample and the amount of TL induced by a unit dose of radiation, one can determine the age of the natural sample from the equation

$$\text{age} = \frac{\text{(archaeologically acquired thermoluminescence)}}{\text{(TL per unit dose)} \times \text{(annual natural dose rate)}} . \qquad (1.1)$$

The age determined in this manner is the time since the amount of TL present in the sample was reset to zero either by firing (in the case of pottery) or by bleaching (in the case of sediments). In practice, however, TL dating is not as simple as it at first appears.

Problems and Some Solutions

There are many problems with this simple method of age determination. Equation 1.1 assumes that the archaeologically acquired TL is the total amount of TL induced in the sample over its lifetime. Shallow traps (see chapter II) are prone to fading, the leakage of charge from the trap over time. If charge has leaked from a trap, the TL measured from that trap will be lower than expected. Thus, only traps deep enough not to experience fading are suitable for dating purposes.

As was mentioned above, equation 1.1 assumes that there is zero TL present in the sample at zero age. This is generally the case since the high temperature used in firing pottery and the long exposure to sunlight when geological sediments are deposited reduce the TL to zero. However, if a piece of pottery was poorly fired there may be some TL left in the piece after firing. In the case of sediments, there is evidence that the TL is not

reduced to zero by exposure to sunlight regardless of the length of the exposure (Spooner, 1987; Spooner *et al.*, 1988). In either case, if the TL is not zero at zero age, the age determined by equation 1.1 will be too large.

The natural TL in a sample is induced by α, β, γ, and cosmic radiation. Since α radiation is highly ionizing, the TL sensitivity to α radiation is generally lower than that for other types of radiation which are all lightly ionizing. In fact, Aitken (1985) claims that in some samples there may be as much as a 50 % reduction in α sensitivity. Therefore, one must be careful to consider this reduced sensitivity when determining the age of a sample.

Pottery and sediments are inhomogeneous materials. TL generally results from mineral inclusions which constitute only a fraction of the total material. The radiation sources are generally separate from these inclusions in the material. Thus, the range of each type of radiation, combined with the particle sizes, will be a factor in determining the dose received from each type of radiation. Again, the reduced α sensitivity will need to be considered when determining the age of a sample.

In order to determine the TL present in deep traps the sample must be heated to high temperatures. When this is done, black body radiation begins to produce a background signal that will make the TL signal hard to observe. In addition, the TL sensitivity of a sample is generally changed when the sample is heated to a high temperature. For these reasons it would be advantageous to be able to determine the archaeologically acquired TL without the need to directly access the charge stored in deep TL traps. Several methods have been developed that achieve this goal.

It is possible to determine the natural dose a sample has received without accessing any deep traps. This is done by exploiting the 'pre-dose effect'. When exposed to a large dose of radiation, the TL sensitivity of a sample will become larger by a factor proportional to the dose received. Thus to determine the natural dose a sample has received, one need simply compare the natural sensitivity to the sensitivity after applying a known dose to the sample in the laboratory. The ratio of the sensitivity increases will equal the ratio of the doses. This effect is evident in all TL peaks so a low temperature peak may be used to determine the natural dose just as well as a high temperature peak.

Phototransferred thermoluminescence (PTTL) dating also allows determination of the natural dose without heating the sample to high temperatures. This method was first investigated by Bailiff (1976). In this method, charge is transferred from the deep traps to shallower traps by illuminating the sample with light. The amount of charge transferred will be proportional to the amount of charge in the deep traps. Therefore, by transferring charge from the deep traps to an empty, shallow trap, and then measuring the TL from this shallow trap, one can measure the relative amount of charge in the deep traps. With the use of a known calibration dose applied in the laboratory, the relative measurement can be converted to an absolute measure of the natural TL.

PTTL has several advantages over other dating methods. As was already mentioned, PTTL does not require the sample to be heated to high temperatures. This allows dating of bone and shell samples which undergo phase changes at the higher temperatures required by other methods. PTTL allows electrons in deep traps which

produce little direct TL due to thermal quenching[1] to be accessed for dating. Another important advantage to PTTL dating is that many measurements can be made on one sample since the sensitivity changes due to heating are avoided and only a small fraction of the electrons in the deep traps are removed for each measurement. This allows dating to be performed on very small samples.

Despite the many advantages, PTTL dating is not widely used at the present time due to several associated problems. For example, in quartz, a common dating material, there are large differences in PTTL sensitivities among different varieties. Also, electrons can be phototransferred easily from some traps while not from others.

In addition to these problems, our lack of understanding of the dynamics of the PTTL effect may contribute to PTTL dating being underutilized. The details of the PTTL process are not widely understood and another method, optically stimulated luminescence (OSL), is available with the same advantages and less unknowns. Until there is a better understanding of the process and perhaps a model which accurately predicts the experimental results, PTTL will not be used much in dating.

Current Topics

Most current research in dating is being conducted on OSL, due to the many advantages OSL has over TL and PTTL as a dating and dosimetry tool. OSL was first

[1] At high temperatures there is a decrease in the efficiency of the TL process. This stems from the increased likelihood that the energy from a recombination process will be dissipated in the form of phonons rather than photons. This effect is known as thermal quenching. Thermal quenching is often observed, but not in all materials. For example, quartz shows thermal quenching, but feldspars do not.

suggested as a dating tool by Huntley *et al.* (1985). Since then, numerous papers have been published on topics ranging from additional applications, such as dosimetry (e.g. Markey *et al.*, 1995), to experimental apparati (e.g. Bøtter-Jensen *et al.* (1994), Pierson *et al.* (1994)). Also, much work has been done to try to understand the OSL process from both a theoretical and experimental point of view. Here PTTL can be of some value.

PTTL and OSL involve identical system dynamics during illumination. Also, PTTL and OSL may result from similar recombination processes. Therefore, a greater understanding of PTTL could lead to a further understanding of OSL. For example, the wavelength response of PTTL will be similar to that for OSL since each depends on the effectiveness of certain wavelengths of light to excite electrons from donor traps.

PTTL also allows the study of shallow traps which, while not directly involved in the OSL process, do have significant effects on the observed OSL. For example, shallow traps are believed to be responsible for a long, non-exponential tail in the OSL decay, and to give rise to a temperature dependence of OSL (McKeever *et al.*, 1996). In addition, shallow traps cause recuperation[2] of the OSL signal (Aitken and Smith, 1988).

Therefore, the study of PTTL is of interest since OSL is so widely used in dating, and so much can be learned about the dynamics of OSL by studying PTTL effects. Quartz is chosen as the material of interest due to its frequent use in dating applications.

[2] With continued exposure to light, the OSL signal will decay. However, electrons which have been phototransferred to shallow traps during illumination can be thermally excited (even at room temperature) to the conduction band and be retrapped in deeper traps responsible for OSL. If the sample is then exposed to light again, the detected OSL signal will be larger than at the end of the previous illumination.

Purpose of Thesis

The purpose of this thesis is to further the understanding of the PTTL process in quartz. Specifically, an analytical description of PTTL will be developed in light of competition effects. Several numerical models will be developed and studied to determine their effectiveness in describing PTTL in quartz, using experimental results as a basis of comparison. Finally, new techniques for analyzing experimental results will be proposed.

CHAPTER II

THEORY

Analytical discussion of the PTTL process requires a basis of elementary concepts and terminology. This basis is established here followed by a detailed analysis of the PTTL arising from a most simple model. Finally, a more complex (and more realistic) model is proposed and analyzed.

Energy Bands and Localized Levels

Theoretical understanding of all luminescent phenomena, including PTTL, is rooted in the energy band crystal model. Energy bands in a crystal arise from the solution of the Schrödinger equation for electrons in a periodic potential. We find that out of the continuous electron energy spectrum, only certain ranges will allow wavelike solutions. These ranges are separated by forbidden regions for which no wavelike electron orbitals exist. These forbidden regions are called band gaps. The allowed ranges are called energy bands.

The number of electrons present in any energy band is described by the equation

$$N(\varepsilon) = D(\varepsilon)\, f(\varepsilon) \tag{2.1}$$

where $D(\varepsilon)$ is the density occupied states and $f(\varepsilon)$ is the Fermi-Dirac distribution function given by

$$f(\varepsilon) = 1/\{\exp[(\varepsilon - \varepsilon_f) / kT] + 1\}. \tag{2.2}$$

The energy ε_f is the Fermi energy. At absolute zero, all energy states below the Fermi level are completely filled and all states above the Fermi level are empty. In semiconductors and insulators, the Fermi level lies above the top valence band and below the bottom conduction band.

Generally, for a perfect semiconductor or insulator, there are no available energy states between the top of the valence band and the bottom of the conduction band. However, if the crystal contains impurities or defects in its periodic lattice, the potential is no longer perfectly periodic. This breakdown in periodicity allows certain electron energies to exist inside the band gaps of the perfect crystal. These energy levels are known as localized levels. The number and exact energy of these levels is determined by the number and type of defects or impurities. Thus, they will depend heavily on the conditions under which the crystal was formed.

To understand how defects and impurities cause localized levels, consider a general M^+X^- semiconductor crystal. An electron which has been freed from the valence band (by irradiation or other means) will wander through the crystal. It may be attracted by the coulombic field of a vacant anion site (a defect of a missing X^- ion) and become weakly bound to that site or 'trapped'. The trapped electron is no longer able to contribute to conduction. Also, the energy required to release this trapped electron is less than the energy required to free an electron from an X^- ion. Thus, the energy associated with the anion vacancy lies somewhere between the valence and conduction bands. Electron traps will lie above the Fermi level. An analogous situation exists for holes trapped by missing M^+ ions. These hole traps will lie below the Fermi level.

Traps and Recombination Centers

Population changes in the various localized levels give rise to luminescent phenomena. These population changes are caused by charge moving among the various levels in a crystal. Figure 2.1 shows several possible transitions for both electrons and holes.

Transition (a) occurs when a valence electron is ionized from its host atom. The electron receives energy from some external source (e.g. radiation) and is excited from the valence band to the conduction band. This process also leaves behind a hole in the valence band. Both the excited electron and the hole are then free to move about in the crystal. There are now several options available to the free charge carriers. First, they may become localized at defect sites. This is the trapping process previously discussed. Transition (b) corresponds to electron trapping and transition (e) corresponds to hole trapping. Another option for the free charges is recombination with a charge carrier of opposite sign. This can occur directly (transition (h)) or indirectly through recombination with a previously trapped charge (transitions (d) and (g)). It is this recombination, when accompanied by the emission of light, which is observed as luminescence.

We can now classify the different localized energy levels as either traps or recombination centers. The important difference between the two is that traps hold charge carriers and then release them to their free state (the conduction band for electrons or the valence band for holes), while recombination centers are, as the name implies, defect sites where recombination of unlike charge carriers occurs. Thus, from figure 2.1, for the

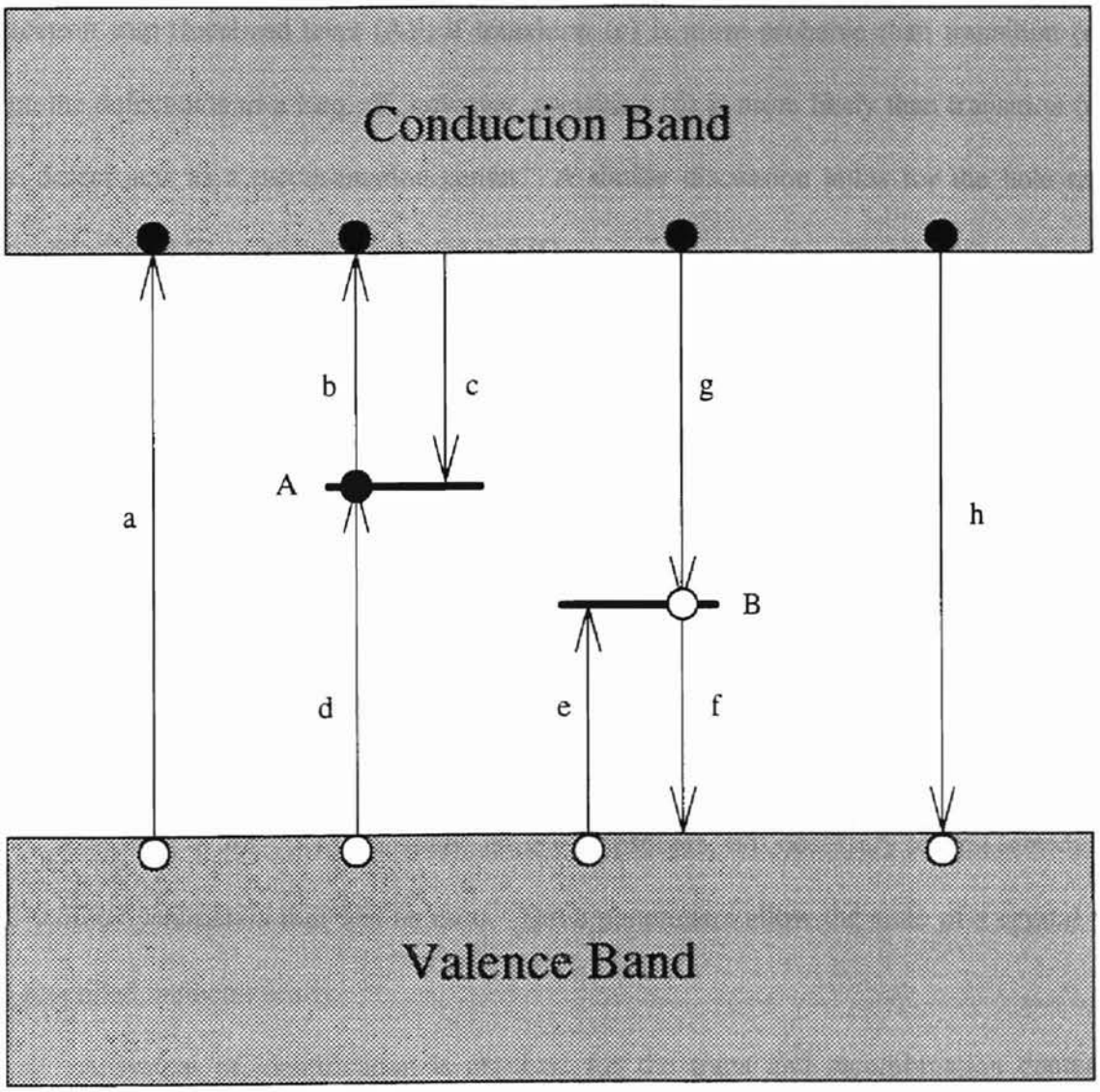

Figure 2.1: Schematic diagram of the possible electron and hole transitions involved in TL and PTTL. Each transition is described in the text. [After McKeever, 1985]

electron trap (localized level (A)), if transition (c) is more probable than transition (d), then the defect acts as a trap. If, however, transition (d) is more likely than transition (c), the defect acts as a recombination center. A similar discussion holds for the hole trap (localized level (B)) and transitions (e) and (f).

Recombination centers can be further classified as either luminescent or non-luminescent. Luminescent recombination centers are those for which the recombination process is accompanied by the emission of light. Non-luminescent recombination centers are those for which the recombination process gives off no detectable light.

Model Parameters

In order to analytically describe the PTTL process, it is necessary to first introduce the various parameters that will be used. These parameters allow the state of a crystal to be described mathematically.

A system of identification is required for the traps and recombination centers. When discussing theoretical models, traps will be indexed by numbers (e.g. 1, 2, 3, ...). Experimentally, traps are often referred to by the relative depth of the traps. The trap depth is the energy required to free a charge carrier from the trap. Thus, traps may be referred to as shallow or deep, where shallow traps have small depths and deep traps have large depths. Experimentally, the charge carriers are usually released by heating a sample. Thus, another common method of labeling the traps is by the temperature at which the

charge carriers have enough thermal energy to be released from the trap. This is related to the trap depth by the 'rule of thumb' approximation

$$E \approx 25\, k\, T \tag{2.3}$$

where E is the trap depth, k is Boltzmann's constant, and T is the absolute temperature (McKeever, 1985). Recombination centers are generally only discussed in relation to theoretical models and will be indexed by numbers preceded with a capital 'R' (e.g. R1, R2, ...). When recombination centers are discussed in relation to experimental data, they will be referred to as luminescent or non-luminescent.

The concentration of any trap will be represented by N_i, where the subscript 'i' is the trap index number. Similarly, recombination centers will be represented by N_{Ri}, where the subscript 'Ri' is the recombination center index number.

The concentration of electrons in trap i will be denoted by n_i. Obviously, this concentration can never be greater than the trap concentration, N_i. The concentration of holes in recombination center Ri will be denoted by m_{Ri}. Again, this concentration can not exceed the recombination center concentration, N_{Ri}. Also, n_c will denote the concentration of electrons in the conduction band and m_v will denote the concentration of holes in the valence band. These two concentrations are assumed to have no upper limits.

In describing the behavior of a crystal, the probabilities of certain transitions are important. The probability of an electron in the conduction band being trapped in trap i will be denoted by A_i. The probability of a hole in the valence band being trapped in recombination center Ri will be denoted by $\hat{A}_{Ri}$. The symbol A_{Ri} will represent the probability of an electron in the conduction band recombining with a hole at recombination

center Ri. The probability of direct combination is generally much smaller than that of indirect recombination and is assumed to be zero.

In order to describe the excitation of an electron from a trap to the conduction band, we need a parameter known as the frequency factor or the attempt to escape frequency. This parameter will be denoted by s_i for trap i.

Description of TL

It is important to have at least a minimal understanding of the TL process in order to understand the more complex PTTL process. In order to observe TL, charge carriers must be ionized. This is usually accomplished by irradiating the sample. Then the sample is heated and TL is observed as a faint glow.

In order to discuss TL in a quantitative manner, a model must first be defined. The simplest model will consist of one trap and one recombination center. This model is shown in figure 2.2. After irradiation, there will be some concentration of electrons in the trap and an equal concentration of holes in the recombination center. If the sample is heated, the electrons in the trap will eventually gain enough thermal energy to escape. When this happens, the electrons will be free to move through the crystal and will eventually either be retrapped in the trap or recombine with holes in the recombination center. When they recombine, the excess energy is given off as photons. This light is the observed TL. The total luminescence signal is denoted by S.

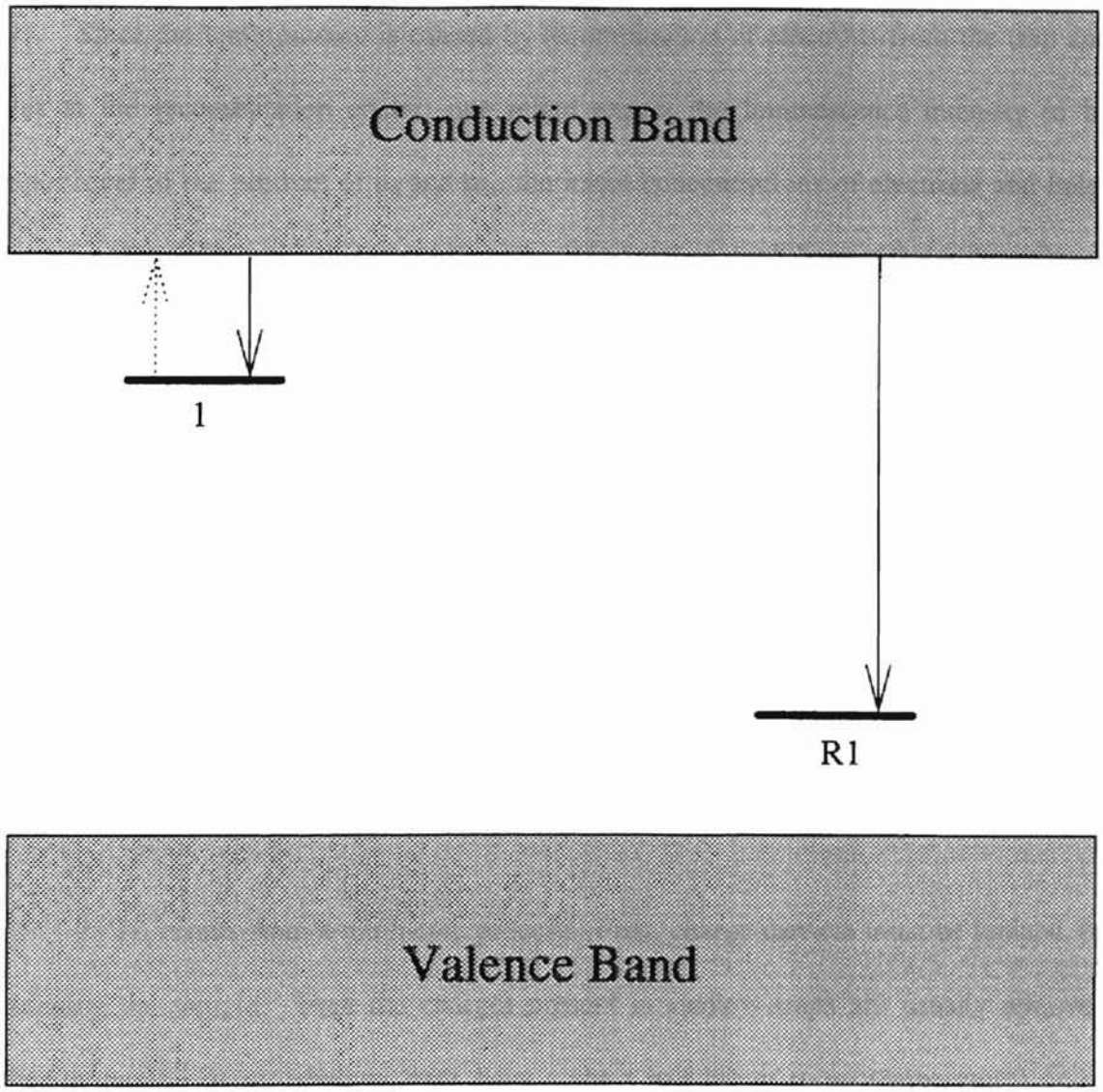

Figure 2.2: Schematic diagram of the band structure of the simplest TL model. Each level is described in the text. Thermal excitation is indicated by a dotted line. Trapping and recombination is indicated by a solid line.

Since the luminescence is caused by recombination of electrons from the trap and holes at the recombination center, one might expect the luminescence intensity to be proportional to the product of n_o and m_o, the initial concentrations of electrons and holes before heating. However, this is not the case. If n_o and m_o both have a linear dependence on dose, which is common, then the product would have a quadratic dependence on dose. It is well known however that TL has a linear or nearly linear dependence on dose. Thus the idea that $S \propto n_o \cdot m_o$ is not valid. However, it can be shown that $S \propto \min(n_o, m_o)$ (Chen and McKeever, 1997). In this simple TL model, $n_o = m_o$, thus $S \propto n_o$ (or m_o) yielding the linear dose dependence.

Description of PTTL

PTTL results from a multi-step process. First, charge carriers must be ionized, by irradiating the sample. Then the charges present in shallow traps are usually removed either by natural decay (shallow traps have a short half life at room temperature) or by heating the sample to a temperature just sufficient to excite charge from the shallow traps but not the deeper traps. If the sample was heated at this point to determine the TL signal, no TL would be detected from the shallow traps. The next step is to expose the sample to stimulation light. The light excites electrons from deep traps into the conduction band from where a proportion will be trapped in the shallow traps. The sample is then heated to determine the TL signal. TL will now be observed from the shallow traps since there is

a non-zero concentration of charge in them. This TL signal is called phototransferred TL or PTTL.

In order to observe PTTL, the sample must have at least two traps. One deep trap to serve as the source of electrons under optical stimulation, and a second shallow trap to receive these electrons. We must also have at least one recombination center in order to allow luminescent recombination. Thus, the simplest model that can be used to describe PTTL contains two traps and one recombination center. This model is shown in figure 2.3. Using this simple model, a mathematical description of the PTTL can be constructed by considering each step in the PTTL process.

The process begins with a virgin sample, one with all traps and recombination centers devoid of charge carriers. Irradiation of the sample leads to a concentration of trapped electrons and holes. The flow of charge during this process can be described by the following equations:

$$dn_c / dt = X - A_1 (N_1 - n_1) n_c - A_2 (N_2 - n_2) n_c - A_{R1} m n_c + \gamma_1 n_1 + \gamma_2 n_2 \qquad (2.4a)$$

$$dn_1 / dt = A_1 (N_1 - n_1) n_c - \gamma_1 n_1 \qquad (2.4b)$$

$$dn_2 / dt = A_2 (N_2 - n_2) n_c - \gamma_2 n_2 \qquad (2.4c)$$

$$dm / dt = \hat{A}_{R1} (N_{R1} - m) n_v - A_{R1} m n_c \qquad (2.4d)$$

$$dn_v / dt = X - \hat{A}_{R1} (N_{R1} - m) n_v \qquad (2.4e)$$

where X is the rate of electron-hole pair generation, and γ_i is probability of thermal excitation from trap i given by

$$\gamma_i = s_i \exp(-E_i / k T) \qquad (2.5)$$

where E_i is the trap depth of trap i and T is the absolute temperature. All other terms are

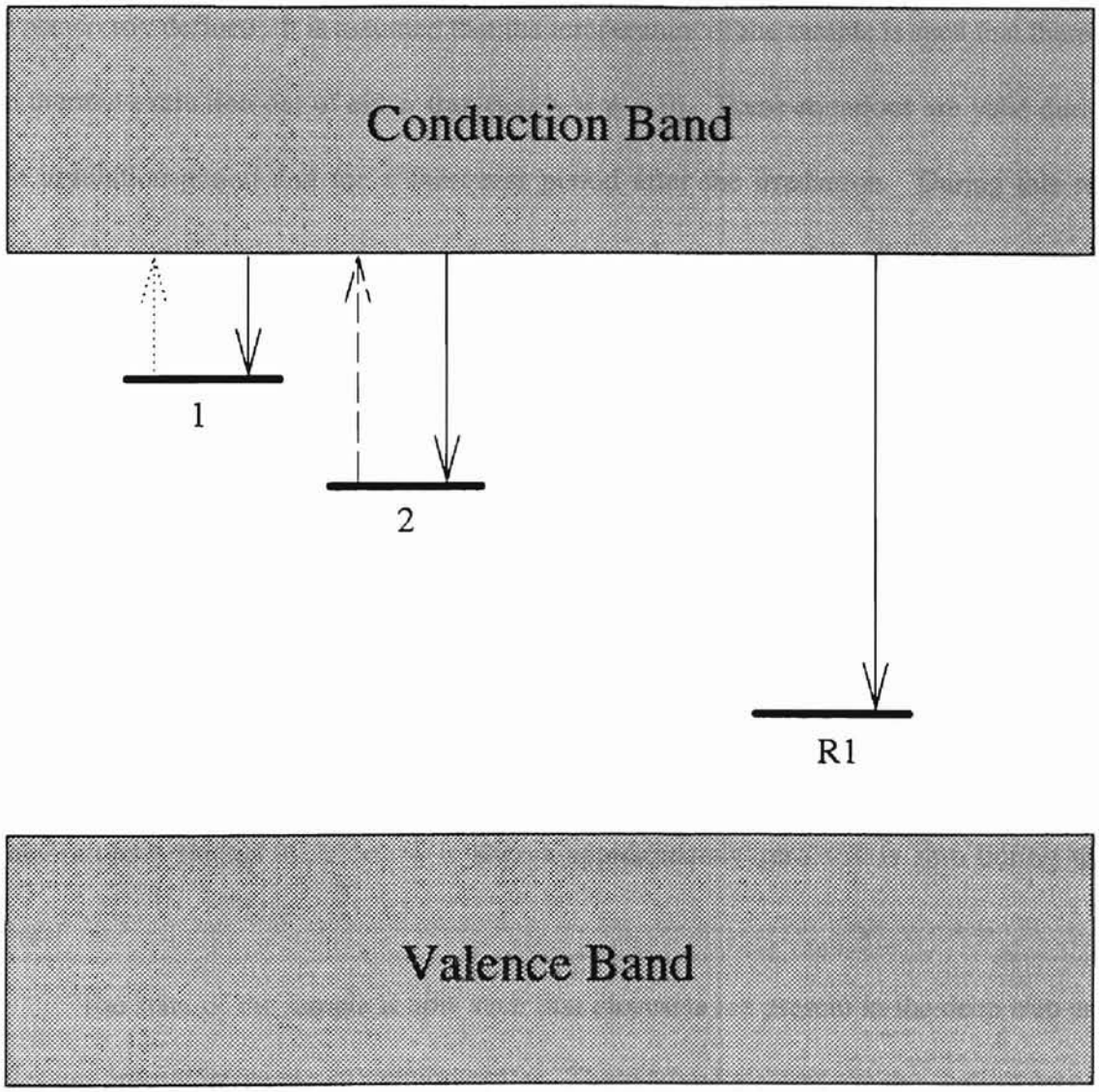

Figure 2.3: Schematic diagram of the band structure of the simplest PTTL model. Each level is described in the text. Thermal excitation is indicated by a dotted line. Optical excitation is indicated by a dashed line. Trapping and recombination is indicated by a solid line.

as previously defined. It is assumed that the temperature of the sample is such that there is no thermal excitation out of either trap (i.e. $\gamma_1 = \gamma_2 = 0$). These equations are valid during the irradiation period and for a short rest period after the irradiation. During this rest period the sample is exposed to no further external energy and is allowed to come to equilibrium. After the rest period it is assumed that there are no electrons in the conduction band nor any holes in the valence band.

Having irradiated the sample, the next step is to remove the charge from the shallow trap. This can be done by leaving the sample at room temperature for sufficient time (this time will vary depending on γ_1). For small γ_1, this time may be excessively long. In this case, the sample is heated to a temperature such that γ_1 is no longer small. If heating is used, this process is then referred to as a pre-heat. It is assumed that the temperature is limited such that γ_2 is always approximately zero. X is zero during this stage.

The state of the sample is now such that electrons are present in the deep trap and holes are present in the recombination center. There are no electrons in the shallow trap.

The sample is now illuminated, usually with monochromatic light. The electrons in the deep trap may absorb these photons and be optically excited into the conduction band. Just as before, these electrons may move through the sample until they become trapped in the shallow trap, retrapped in the deep trap, or recombine with holes in the recombination center. The light given off by the recombinations during illumination is known as optically stimulated luminescence (OSL). The important point in considering PTTL is that electrons have been moved or *phototransferred* from the deep trap to the shallow trap.

During the illumination phase, the flow of charge can be described by the following equations:

$$dn_c / dt = - dn_1 / dt - dn_2 / dt + dm / dt \quad (2.6a)$$

$$dn_1 / dt = A_1 (N_1 - n_1) n_c \quad (2.6b)$$

$$dn_2 / dt = A_2 (N_2 - n_2) n_c - f \sigma n_2 \quad (2.6c)$$

$$dm / dt = - A_{R1} m n_c \quad (2.6d)$$

$$dn_v / dt = 0 \quad (2.6e)$$

where f is the intensity of the photon flux and σ is the photoionization cross section for electrons in the deep trap and all other terms are as previously defined. Again, it is assumed that the sample temperature is such that there is no thermal excitation from either trap. Also, it is generally assumed that the sample remains in quasi-equilibrium during illumination. That is, that dn_c / dt is approximately zero at all times. This assumption simply means that the rate of excitation is the same as the rate of trapping and recombination.

After illumination the sample again has electrons in both traps. The electrons in the shallow trap will give rise to the PTTL signal.

In order to observe the PTTL signal, the sample is now heated. During heating electrons will be thermally released from the traps. Electrons released from the shallow trap will either recombine with holes in the recombination center or be trapped in the deep trap which will be thermally stable while the shallow trap is thermally unstable. The flow of charge during the heating process can be described by the following equations:

$$dn_c / dt = - dn_1 / dt - dn_2 / dt + dm / dt \quad (2.7a)$$

$$dn_1 / dt = A_1 (N_1 - n_1) n_c - \gamma_1 n_1 \quad (2.7b)$$

$$dn_2 / dt = A_2 (N_2 - n_2) n_c - \gamma_2 n_2 \quad (2.7c)$$

$$dm / dt = - A_{R1} m n_c \quad (2.7d)$$

$$dn_v / dt = 0 \quad (2.7e)$$

where all terms are as previously defined. Again we assume quasi-equilibrium so

$$dn_c / dt \approx 0. \quad (2.8)$$

Thus, equation 2.7a becomes

$$dm / dt = dn_1 / dt + dn_2 / dt. \quad (2.9)$$

This model can be used to predict the expected PTTL signal for a given set of parameters. The intensity of the luminescence signal observed is denoted by I(t) where t represents time. It is assumed that the sample is heated linearly with respect to time so that time is proportional to temperature. Chen and McKeever (1997) analytically solve the set of equations 2.7 with 2.9 for I(t) to yield

$$I(t) = \gamma A_m m F(m) \quad (2.10)$$

where

$$F(m) = \frac{(n_{1o} + n_{2o} - m_o - N_2) + m + (N_2 - n_{2o})(m / m_o)^{A_2/A_m}}{A_1 (N_1 + N_2 - n_{1o} - n_{2o} + m_o) + (A_m - A_1)(N_2 - n_{2o})(m / m_o)^{A_2/A_m}}. \quad (2.11)$$

This equation can be numerically evaluated for various sets of parameters. This expression was derived with only two assumptions. Namely, quasi-equilibrium and that the temperature is always low enough that γ_2 is approximately zero. If further assumptions are made, equation 2.11 can be integrated to give the final value of the

concentration of holes in the recombination center, m_∞. This value can then be used to find the total luminescence, denoted by S, since

$$S = m_o - m_\infty.$$

For example, if we assume that trapping in trap 2 is much faster than recombination, that at the start of heating $n_{1o} \ll N_2 - n_{2o}$, and that retrapping into trap 1 is negligible (i.e. trapping into trap 2 dominates the competition) then

$$S = [A_m / A_2 (N_2 - n_{2o})] m_o n_{1o}. \qquad (2.12)$$

Other sets of assumptions lead to similar equations.

One important observation about equation 2.12 is that $S \propto n_o \cdot m_o$. Thus S is no longer proportional to the minimum of n_{1o} and m_o as discussed above. This is because we no longer are dealing with a model where electrons, once excited to the conduction band, can only be retrapped or recombine. Here electrons can also be trapped in the second trap. Since trap 2 will be thermally stable at temperatures where trap 1 is not, trap 2 will act as an effective competitor. That is, both trap 2 and the recombination center will be competing for the available electrons. When this occurs, the model is called a competition model and we no longer find S to be proportional to the minimum of n_{1o} and m_o.

While this simple model can describe all of the essential features of the PTTL process, it will be shown in the next chapter that it does not accurately predict experimental data. A more complex model is needed. As a first step towards a more realistic model, a second non-luminescent recombination center was added. The resulting model is shown in figure 2.4. The model is described mathematically in a similar fashion to that used for the simple model.

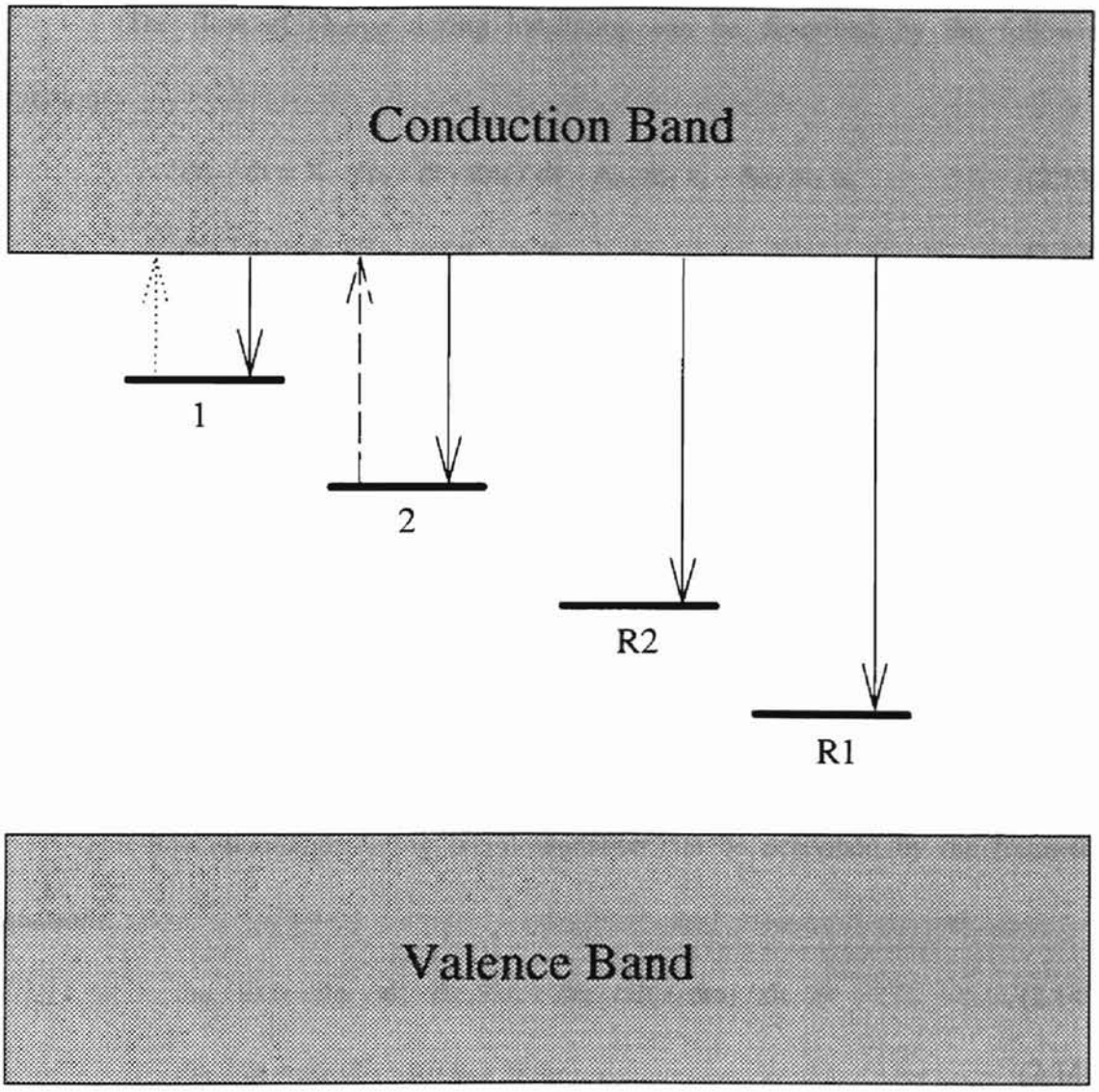

Figure 2.4: Schematic diagram of the band structure of the more complex PTTL model. Each level is described in the text. Thermal excitation is indicated by a dotted line. Optical excitation is indicated by a dashed line. Trapping and recombination is indicated by a solid line.

The flow of charge during irradiation can be described by the following equations:

$$dn_c / dt = X - dn_1 / dt - dn_2 / dt - A_{R1} m_1 n_c - A_{R2} m_2 n_c \quad (2.13a)$$

$$dn_1 / dt = A_1 (N_1 - n_1) n_c - \gamma_1 n_1 \quad (2.13b)$$

$$dn_2 / dt = A_2 (N_2 - n_2) n_c - \gamma_2 n_2 \quad (2.13c)$$

$$dm_1 / dt = \hat{A}_{R1} (N_{R1} - m_1) n_v - A_{R1} m_1 n_c \quad (2.13d)$$

$$dm_2 / dt = \hat{A}_{R2} (N_{R2} - m_2) n_v - A_{R2} m_2 n_c \quad (2.13e)$$

$$dn_v / dt = X - \hat{A}_{R1} (N_{R1} - m_1) n_v - \hat{A}_{R2} (N_{R2} - m_2) n_v \quad (2.13f)$$

where all terms are as previously defined. These equations are valid during the irradiation period and for a short rest period after the irradiation while the sample comes to equilibrium.

The flow of charge during the illumination can be described by the following equations:

$$dn_c / dt = - dn_1 / dt - dn_2 / dt + dm_1 / dt + dm_2 / dt \quad (2.14a)$$

$$dn_1 / dt = A_1 (N_1 - n_1) n_c - \gamma_1 n_1 \quad (2.14b)$$

$$dn_2 / dt = A_2 (N_2 - n_2) n_c - \gamma_2 n_2 - f \sigma n_2 \quad (2.14c)$$

$$dm_1 / dt = - A_{R1} m_1 n_c \quad (2.14d)$$

$$dm_2 / dt = - A_{R2} m_2 n_c \quad (2.14e)$$

$$dn_v / dt = 0 \quad (2.14f)$$

where all terms are as previously defined. Again, it is assumed that the sample remains in quasi-equilibrium ($dn_c / dt \approx 0$) during illumination, and that the illumination is done at a temperature such that $\gamma_1 = \gamma_2 \approx 0$.

The heating process can be described by the following equations:

$$dn_c / dt = - dn_1 / dt - dn_2 / dt + dm_1 / dt + dm_2 / dt \quad (2.15a)$$

$$dn_1 / dt = A_1 (N_1 - n_1) n_c - \gamma_1 n_1 \quad (2.15b)$$

$$dn_2 / dt = A_2 (N_2 - n_2) n_c - \gamma_2 n_2 \quad (2.15c)$$

$$dm_1 / dt = - A_{R1} m_1 n_c \quad (2.15d)$$

$$dm_2 / dt = - A_{R2} m_2 n_c \quad (2.15e)$$

$$dn_v / dt = 0 \quad (2.15f)$$

where all terms are as previously defined. Again, we assume quasi-equilibrium,

$$dn_c / dt \approx 0. \quad (2.16)$$

Thus, equation 2.15a becomes

$$dm_1 / dt + dm_2 / dt = dn_1 / dt + dn_2 / dt. \quad (2.17)$$

This model can be used to predict experimental results with better accuracy than the simple model. Following a similar procedure to that used by Chen and McKeever (1997) for the simple model, we find an explicit expression for the PTTL intensity, I(t), during heating.

First, one must observe that the PTTL signal is caused by recombinations occurring at recombination center R1. Since each recombination will emit the same amount of light, and the number of recombinations is proportional to the absolute rate of change of the charge concentration in R1, $| dm_1 / dt |$, the PTTL intensity will be proportional to the absolute rate of change of m_1. Also since the concentration m_1 is always decreasing, I(t) will be proportional to the negative of dm_1 / dt. Thus we have:

$$I(t) = -dm_1 / dt = A_{R1} m_1 n_c. \quad (2.18)$$

The first equality is valid since I(t) is only relevant up to a scaling factor. The second equality comes from equation 2.15d.

Substituting equations 2.15b, 2.15c, 2.15e, and 2.18 into 2.17 and solving for n_c, one finds

$$n_c = \gamma_1 n_1 / \{m_1 A_{R1} + m_2 A_{R2} + (N_1 - n_1) A_1 + (N_2 - n_2) A_2\}. \quad (2.19)$$

Substituting 2.19 into 2.18, one finds

$$I(t) = \gamma_1 n_1 m_1 A_{R1} / \{ m_1 A_{R1} + m_2 A_{R2} + (N_1 - n_1) A_1 + (N_2 - n_2) A_2\}. \quad (2.20)$$

Now, using equations 2.15c and 2.18, one gets

$$n_c = \frac{1}{A_2}\frac{d}{dt}\ln(N_2 - n_2) = \frac{1}{A_{R1}}\frac{d}{dt}\ln(m_1) \quad (2.21)$$

which can be integrated to give

$$N_2 - n_2 = (N_2 - n_{2o})(m_1 / m_{1o})^{A_2/A_{R1}}. \quad (2.22)$$

Similarly, from 2.18 and 2.15e, one finds

$$n_c = \frac{1}{A_{R2}}\frac{d}{dt}\ln(m_2) = \frac{1}{A_{R1}}\frac{d}{dt}\ln(m_1) \quad (2.23)$$

which can be integrated to give

$$m_2 = m_{2o}(m_1 / m_{1o})^{A_{R2}/A_{R1}}. \quad (2.24)$$

Integration of 2.17 yields

$$m_1 - m_{1o} = n_1 - n_{1o} + n_2 - n_{2o} - m_2 + m_{2o}. \quad (2.25)$$

Solving 2.25 for n_1 gives

$$n_1 = m_1 - m_{1o} + n_{1o} - n_2 + n_{2o} + m_2 - m_{2o}. \quad (2.26)$$

Substituting 2.22, 2.24, and 2.26 into 2.20 gives

$$I(t) = -dm_1 / dt = \gamma_1 m_1 A_{R1} F(m_1) \tag{2.27}$$

where

$$F(m_1) = \frac{\begin{array}{c} m_1 - m_{1o} + n_{1o} - N_2 + (N_2 - n_{2o})(m_1 / m_{1o})^{A_2/A_{R1}} + \\ n_{2o} + m_{2o}(m_1 / m_{1o})^{A_{R2}/A_{R1}} - m_{2o} \end{array}}{\begin{array}{c} m_1 A_{R1} + m_{2o} A_{R2}(m_1 / m_{1o})^{A_{R2}/A_{R1}} + A_{R2}(N_2 - n_{2o})(m_1 / m_{1o})^{A_2/A_{R1}} + \\ A_{R1}(N_1 - m_1 + m_{1o} - n_{1o} + N_2 - (N_2 - n_{2o})(m_1 / m_{1o})^{A_2/A_{R1}} - \\ n_{2o} - m_{2o}(m_1 / m_{1o})^{A_{R2}/A_{R1}} + m_{2o}) \end{array}}. \tag{2.28}$$

This equation can be evaluated for a given set of parameters.

If it is assumed that excitation out of trap 1 is much faster than retrapping in trap 1, then equation 2.15b becomes

$$dn_1 / dt = -\gamma_1 n_1 \tag{2.29}$$

the solution of which is

$$n_1 = n_{1o} \exp\left(-\int_0^t \gamma d\tau \right). \tag{2.30}$$

If it is also assumed that retrapping into trap 1 is negligible, then 2.27 becomes, with 2.28 and 2.30

$$I(t) = -\frac{dm_1}{dt} = \frac{\gamma_1 m_1 A_{R1} n_{1o} \exp\left(-\int_0^t \gamma d\tau \right)}{m_1 A_{R1} + m_{2o} A_{R2}(m_1 / m_{1o})^{A_{R2}/A_{R1}} + A_{R2}(N_2 - n_{2o})(m_1 / m_{1o})^{A_2/A_{R1}}}. \tag{2.31}$$

If it is then further assumed that trapping into trap 2 is the dominant competition factor, then the first and third terms in the denominator of 2.31 can be neglected. Then equation 2.31 can be integrated to give

$$S = m_{1o}\left(1-\left(1-\frac{n_{1o}}{m_{2o}}\right)^{A_{R1}/A_{R2}}\right) \tag{2.32}$$

where S is the total amount of PTTL produced given concentrations m_{1o}, n_{1o}, and m_{2o} at the start of heating. If instead it is assumed that trapping into recombination center 2 is the dominant competition factor, then the first and second terms in the denominator of 2.31 can be neglected. Integration of 2.13 in this case leads to the equation

$$S = m_{1o}\left(1-\left(1-\frac{n_{1o}}{N_2 - n_{2o}}\right)^{A_{R1}/A_2}\right) \tag{2.33}$$

While each of these equations may seem to be far removed from the actual case due to the many assumptions that were made, it can be shown that this is not the case, at least for some sets of model parameters.

Comparison of Analytical to Numerical Solutions

The differential equations describing both the simple model and the more complex model can be solved numerically. This is described in detail in chapter III. These solutions provide the PTTL intensity as a function of both illumination time and heating temperature.

In order to test the validity of equations 2.10 and 2.27 for the simple and complex models, respectively, these equations were evaluated using the sets of parameters described in chapter III. These results were then compared to the PTTL intensity found from numerical solution of the differential equations. Since the numerical solution of the

differential equations does not involve any assumptions or approximations (other than rounding errors), these results are considered to be more accurate that the analytical solutions which involve assumptions and approximations. The results are shown in figures 2.5 and 2.6. From the figures, it is clear that equations 2.10 and 2.27 are valid since the predictions of these equations are nearly identical to the actual results obtained from a numerical solution of the differential equations. This is not a surprising result, since there were few assumptions made in determining equations 2.10 and 2.27.

While equations 2.10 and 2.27 are important in that they show that the mathematical procedure followed was in fact valid, they are not very useful as an analytical tool. In order to apply these equations, one must have *a priori* knowledge of the concentration of holes in the luminescent recombination center during the heating phase (m in 2.10 or m_{R1} in 2.27). Thus, one must already know the resultant PTTL in order to be able to analytically describe it. Equations 2.12, 2.32, and 2.33 would be more useful since they predict the PTTL that would arise from heating a sample knowing the various charge concentrations at the end of illumination, before heating. Their utility is limited however, since experimentally, these concentrations, as well as the total trap concentrations are not likely to be known.

In order to test the validity of equations 2.12, 2.32, and 2.33, the differential equations describing both models were numerically solved. Using the results from these solutions to determine the charge concentrations after illumination for 0 to 100 s, equations 2.12, 2.32, and 2.33 were used to predict the PTTL that would result if illumination was stopped and the sample was heated. These results and the PTTL results from the numerical solution of the differential equations are shown in figures 2.7 and 2.8.

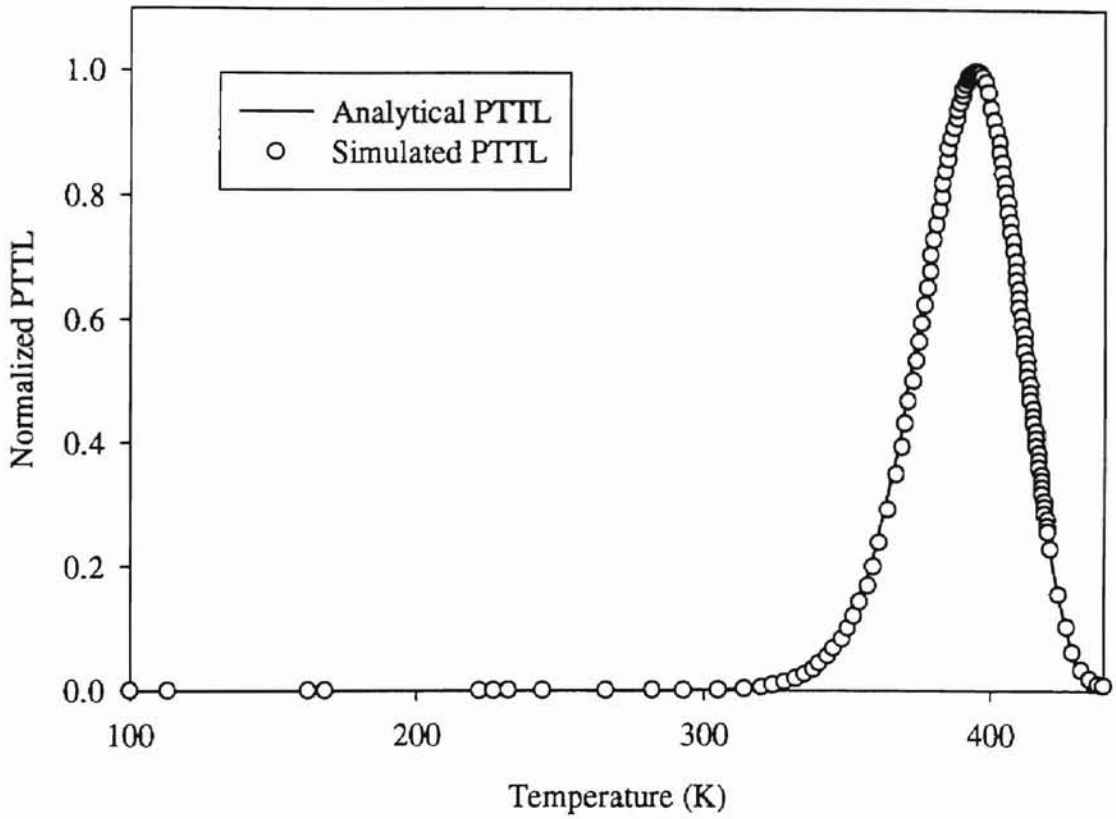

Figure 2.5: Analytically calculated PTTL (equation 2.10) is shown along with the numerically simulated PTTL data for the simple model.

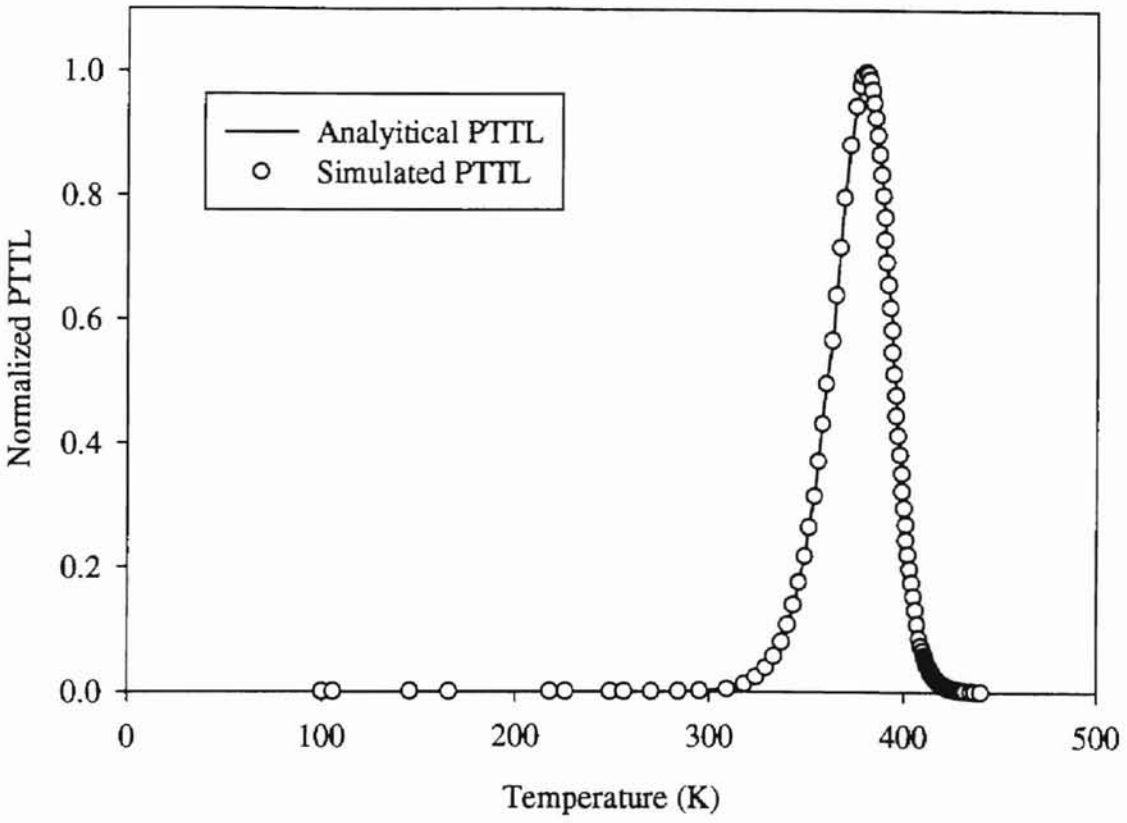

Figure 2.6: Analytically calculated PTTL (equation 2.27) is shown along with the numerically simulated PTTL data for the more complex model.

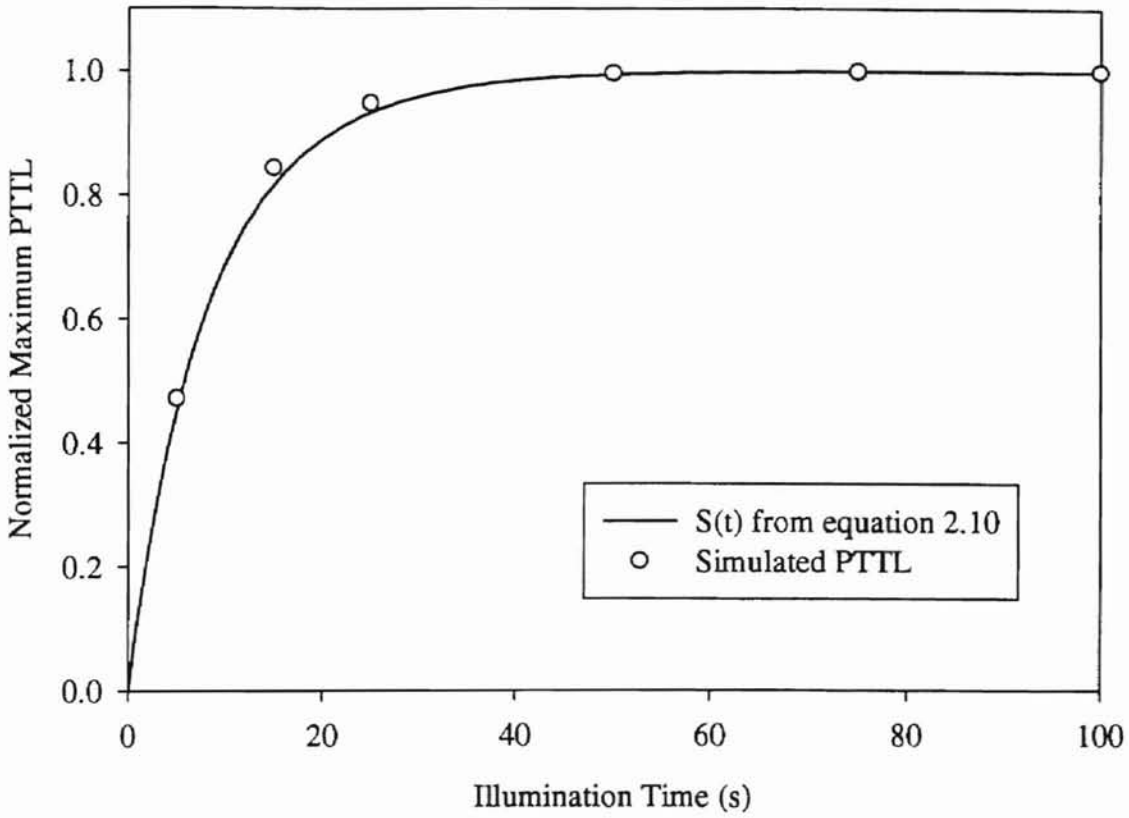

Figure 2.7: The analytically predicted PTTL time response for the simple model using equation 2.10 is plotted along with the numerically simulated PTTL time response for the same model found by direct numeric solution of equations 2.6 - 2.9.

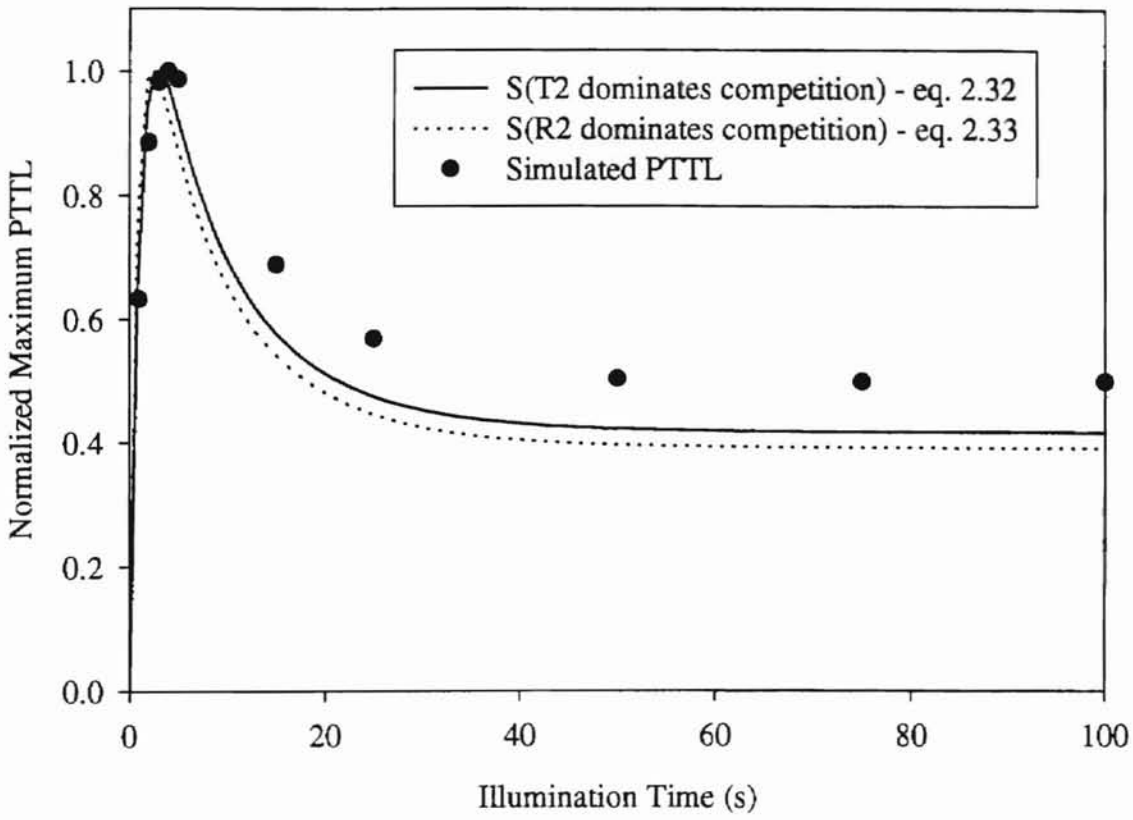

Figure 2.8: The analytically predicted PTTL time response for the more complex model using equations 2.32 and 2.33 is plotted along with the simulated PTTL time response for the same model found by direct numeric solution of equations 2.13 - 2.17.

The figures show that while the equations do not predict exactly the same PTTL that is found from the numerical solutions, they do approximate the results of the numerical solutions. The discrepancy is caused by the assumptions made in deriving equations 2.12, 2.32, and 2.33. Thus, equations 2.12, 2.32, and 2.33 can be used as an analytical tool as long as one remembers that the solutions are not exact, but only approximations of the exact solutions.

Summary and Conclusions of Chapter II

The theoretical background for describing PTTL has been introduced. Two models for PTTL production have been described. These models have been analytically described at several levels of assumption.

Equations 2.10 and 2.27 for the PTTL intensity as a function of heating time are nearly exact solutions when compared to the simulated results of chapter III. These equations are not extremely useful analytical tools however due to the variables present. Equations 2.12, 2.32, and 2.33 are more useful analytically, but less exact due to the additional assumptions required in their derivation.

The agreement shown here between the analytical and numerical solutions should not be taken as a general result. The agreement is for the sets of parameters used only. These parameters are such that the assumptions made were valid. Other sets of parameters may invalidate the assumptions and thus not produce agreement between the numerical and analytical results.

CHAPTER III

NUMERICAL SIMULATIONS

The numerical models of how a sample will respond to the PTTL process can be solved numerically. In this chapter, both the simple model and the more complex model from chapter II are solved numerically. The sensitivity of these models to changes in various parameters is examined. Also, using a third model, the effect of the wavelength of the light used to stimulate the sample on the PTTL signal is examined.

All of the simulations conducted for this thesis were done using RATE, a specialized software package developed at Risø National Laboratory in Denmark. The program was run on an IBM compatible personal computer. The calculations are based on the differential equations presented in chapter II.

Sensitivity Analysis of the Simple Model

The simple model, described in detail in chapter II, consists of two traps and one recombination center. It is described by the set of equations 2.4 through 2.9. This model is shown in figure 2.3.

For this sensitivity analysis, a standard set of parameters was chosen. These parameters were loosely based on a set of parameters used by McKeever (1991) which has shown some promising results (Morris and McKeever, 1994) in attempts to simulate experimental data from quartz. The standard set of parameters used is shown in table 3.1.

In order to simulate the PTTL process, the following steps were used. First, the 'sample' was irradiated for 100 seconds at 290 K with the electron-hole generation rate, X, set to 10^8 s^{-1}. This was followed by a 10 second rest period. Then the 'sample' was pre-heated to 415 K at 8.333 K/s. The 'sample' was held at 415 K for 100 s then cooled to 100 K at -8.333 K/s. The 'sample' was then illuminated for various lengths of time ranging from 5 s to 100 s with the optical excitation rate, $f\sigma$, set to 10^{-1} s^{-1}. To produce the PTTL signal, the 'sample' was then heated to 550 K at 8.333 K/s. The luminescent intensity was calculated from

$$I(t) = A_{R1}\, n_c(t)\, m(t).$$

The results are shown in figures 3.1 and 3.2 where the simulated peak PTTL intensity is plotted verses the length of the illumination period.

From the figures, there is one immediate conclusion. The PTTL produced with this model is monotonically increasing with illumination time. It will be shown later that experimentally, the PTTL is not monotonically increasing but rather shows an increase followed by a decrease to a steady state level. Thus, this model is not consistent with experimental results. Despite this, this model can be useful. The benefit of this simple model is that it allows examination of the effects of each parameter without the complications required to more closely simulate experimental results.

In figure 3.1, the effect of changing the concentration of one trap or recombination center is shown. Considering trap 2, one expects that increasing the concentration will cause an increase in the PTTL signal. To see why, consider each step of the PTTL process. During irradiation, increasing the concentration of trap 2 increases the likelihood that electrons will be trapped there, resulting in more available electrons in the trap. Pre-

Table 3.1
Standard Parameters for the Simple Model

Center	Concentration (cm^{-3})	Trap Depth (eV)	Frequency Factor (s^{-1})	Trapping Probability	Recombination Probability
1	10^{11}	0.90	$5x10^{11}$	10^{-9}	---
2	10^{11}	1.42	10^{14}	10^{-10}	---
R1	10^{11}	---	---	10^{-9}	10^{-7}

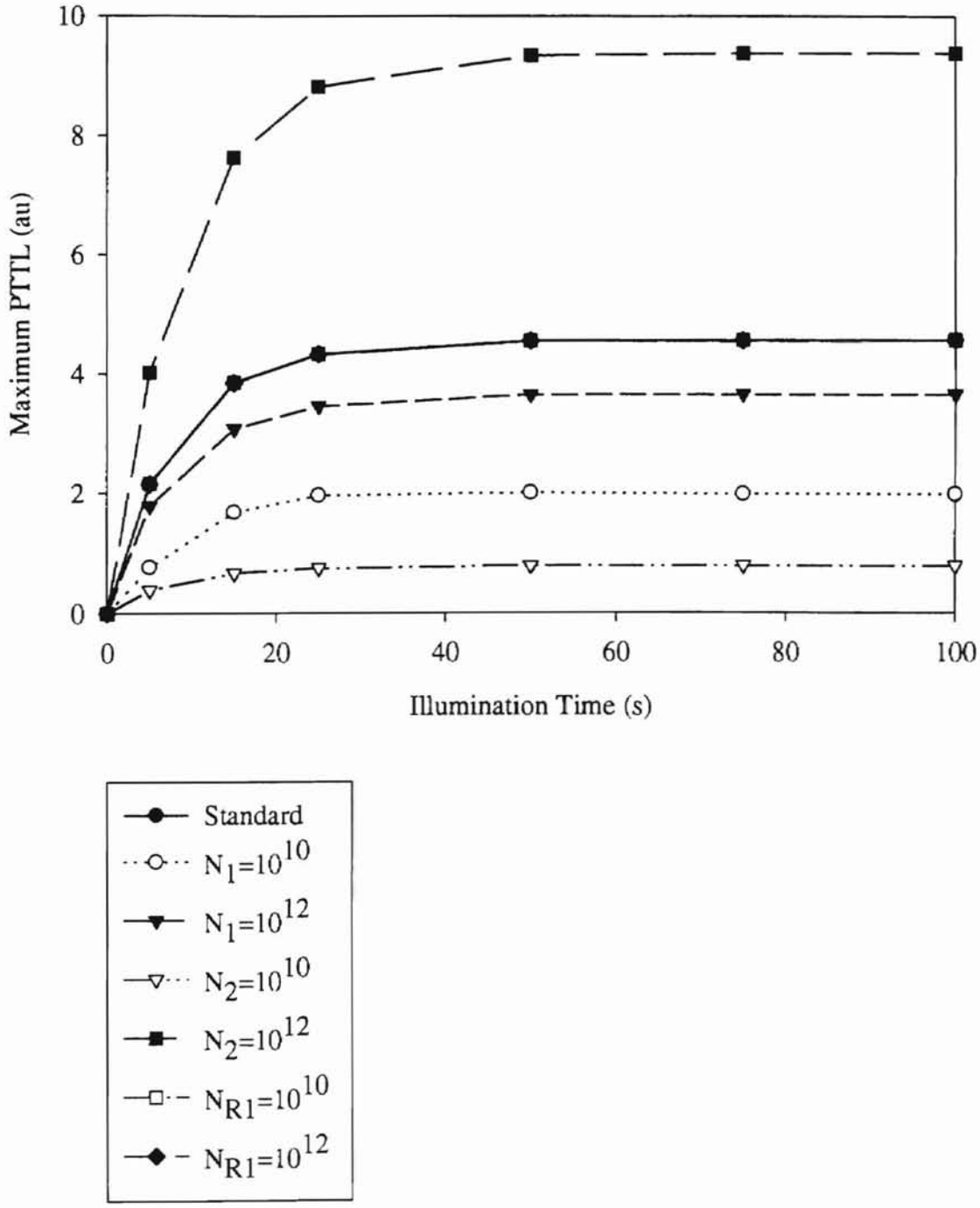

Figure 3.1: Numerically simulated PTTL time response for the model of figure 2.3. Each curve represents a change in the trap or recombination center concentration indicated.

heating does not effect electrons in this trap since the temperature remains low enough that this trap is thermally stable. While the sample is being illuminated, electrons from trap 2 are transferred to trap 1 to become the source of the PTTL signal. Since more electrons are available in trap 2 to be transferred, the final electron concentration in trap 1 will be higher, and more PTTL will be observed. This same argument can be applied in the negative sense to support the conclusion that decreasing the concentration of trap 2 will decrease the PTTL observed. From figure 3.1, we find that both of these expectations are supported.

Now consider trap 1. During the entire PTTL process, changing the concentration of trap 1 will affect two events. During irradiation, trap 1 competes with trap 2 for electrons from the conduction band. Increasing the concentration of trap 1 increases the competition, therefore, more electrons are trapped in trap 1 and fewer in trap 2. This will cause a decrease in the PTTL signal. However, during illumination, an increase in the concentration of trap 1 will increase the probability that photoexcited electrons in the conduction band will be trapped there rather than being retrapped in trap 2 or recombining. This will cause an increase in the PTTL signal. Thus, increasing the concentration of trap 1 can cause both an increase and a decrease in the PTTL signal. The same arguments can be applied in the negative sense to show that decreasing the concentration of trap 1 can also cause both an increase and a decrease in the PTTL signal. These two contradictory effects will compete and the dominant one will be observed in the data. Which effect dominates will depend on the values chosen for the various model

parameters. Figure 3.1 shows, for the parameters chosen for this study, increasing and decreasing the concentration of trap 1 both cause a decrease in the PTTL signal.

From figure 3.1, one finds that changing the concentration of the recombination center had no effect on the size of the PTTL signal. This is most likely due to the fact that the total number of free electrons must equal the total number of free holes. Thus, regardless of the recombination center concentration, there will always be a hole available for an electron wishing to recombine. The recombination center concentration will affect the likelihood of electrons recombining rather than being trapped during irradiation and illumination, however, these competition effects appear to be negligible in the range of recombination center concentrations studied.

In addition to varying the concentrations, the trapping and recombination probabilities were changed. The results are shown in figure 3.2. In the cases of traps 1 and 2, similar results were seen when the trapping probabilities were changed as when the concentrations were changed. This result is not surprising. Increasing or decreasing the concentrations will increase or decrease the trapping probabilities since having more or less trapping sites will make it more or less likely that an electron will be trapped in one. In fact, the numerical values of the PTTL obtained were nearly identical regardless of whether the concentration or the probability was changed. However, this was not the case for the recombination center. When the recombination center hole trapping probability was changed, no change was seen in the PTTL. This can be understood similarly to the case of changing the recombination center concentration. Since there is always a hole available for an electron to recombine with, it does not matter how likely the holes are to be trapped in the recombination center as long as it is not a negligible value. Given

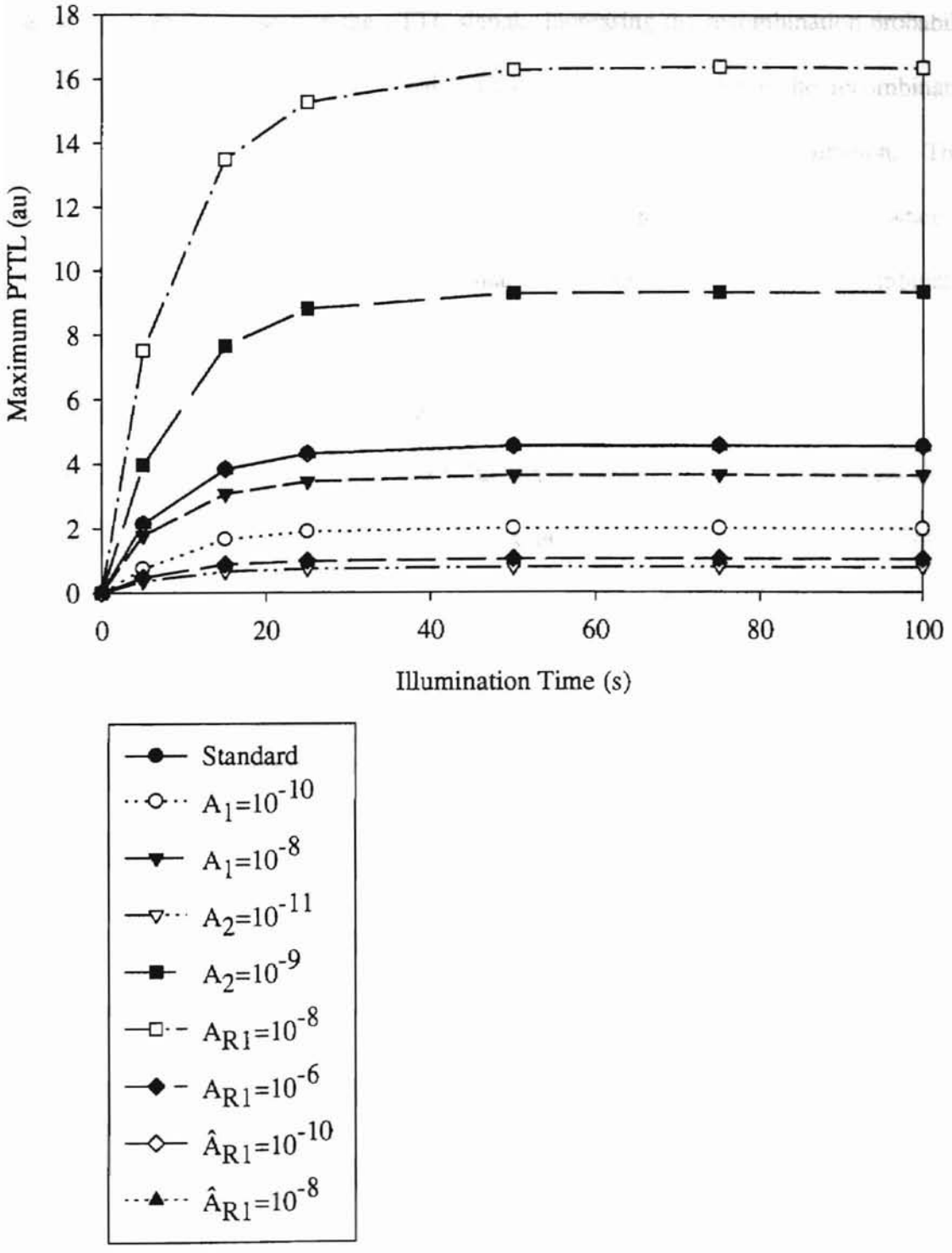

Figure 3.2: Numerically simulated PTTL time response for the model of figure 2.3. Each curve represents a change in the transition probability indicated.

enough time, the holes will be trapped. However, when the recombination probability was changed, a change was seen in the PTTL signal. Increasing the recombination probability caused a decrease in the PTTL signal. This is because increasing the recombination probability increases the competition effect during irradiation and illumination. Thus, fewer electrons are trapped in both traps causing fewer electrons to be in trap 1 when the sample is heated to measure the PTTL signal. Similarly, decreasing the recombination probability decreases the competition and allows more electrons to be trapped in the traps. Thus, the observed PTTL signal is larger.

At this point, one may ask what value this information has since the effect on the PTTL signal could not be predicted but only explained. The value is that as the model is made more complex, many of the same effects will be seen. Since we now know how this simple model reacts to changes in the different parameters, we have a general idea of how to cause certain changes in the PTTL signal in the more complex models. This can be useful when trying to construct a model that accurately predicts experimental results.

Sensitivity Analysis of the More Complex Model

In an attempt to construct a model that more accurately predicts experimental results, a second non-luminescent recombination center was added to the simple model. The new model was described in detail in chapter II. The addition of a second recombination center changes the internal system dynamics at every stage of the PTTL

process. Thus, in order to better understand the model, a sensitivity analysis was conducted on this more complex model.

This model is described by equations 2.13 - 2.17. It is shown in figure 2.4. The standard set of parameters were again based on those used by McKeever (1991) and are shown in table 3.2.

The same sequence of events was used to produce the PTTL signal. Namely, the 'sample' was irradiated for 100 seconds at 290 K with the electron-hole generation rate, X, set to 10^8 s^{-1}. This was followed by a 10 second rest period. Then the 'sample' was pre-heated to 415 K at 8.333 K/s. The 'sample' was held at 415 K for 100 s, then cooled to 100 K at -8.333 K/s. The 'sample' was then illuminated for various lengths of time ranging from 5 s to 100 s with the optical excitation rate, $f\sigma$, set to 10^{-1} s^{-1}. To produce the PTTL signal the 'sample' was then heated to 550 K at 8.333 K/s.

The resulting peak PTTL intensities verses illumination time are shown in figure 3.3. Immediately one can observe that some of the parameter sets produced a PTTL signal that was monotonically increasing with respect to illumination time. However, other sets of parameters show an increase in PTTL followed by a decrease. Thus, the addition of a second non-luminescent recombination center allows the model to predict PTTL verses illumination time with the same basic shape as experimental data.

In this model, some of the effects are similar to those in the simple model. Again we see that increasing or decreasing the concentration of a trap produces nearly identical PTTL signals to those obtained by increasing or decreasing the trapping probability for that trap. Thus, many of the parameter sets will be discussed in pairs.

Table 3.2
Standard Parameters for the More Complex Model

Center	Concentration (cm^{-3})	Trap Depth (eV)	Frequency Factor (s^{-1})	Trapping Probability	Recombination Probability
1	10^{11}	0.90	$5x10^{11}$	10^{-9}	---
2	10^{11}	1.42	10^{14}	10^{-10}	---
R1	10^{11}	---	---	10^{-9}	10^{-7}
R2	10^{11}	---	---	10^{-9}	10^{-8}

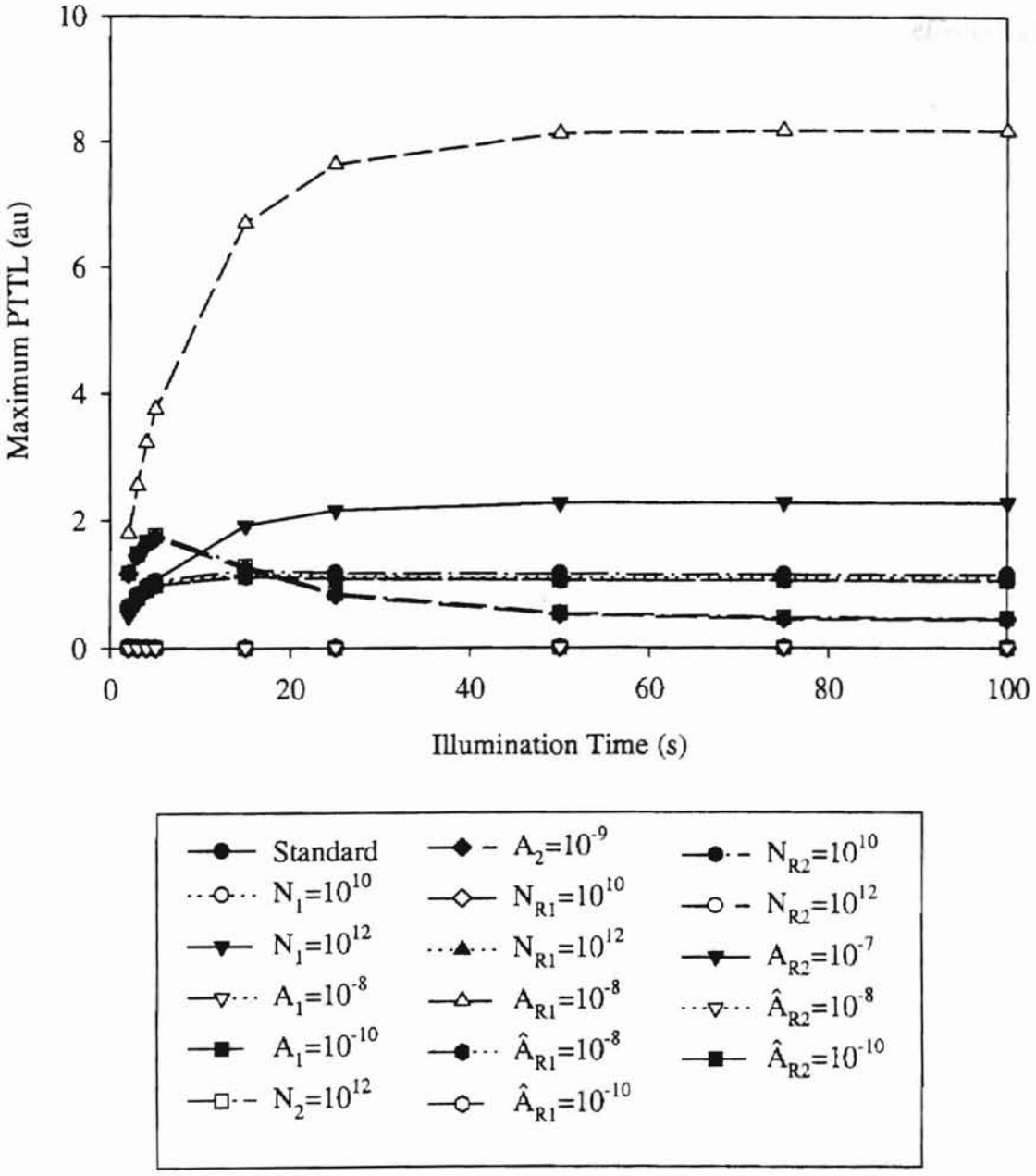

Figure 3.3: Numerically simulated PTTL time response for the model of figure 2.4. Each curve represents a change in the parameter indicated.

From the simple model analysis, we know that the changes caused by each individual parameter can not be predicted but only explained. Therefore, the effect of each parameter will not be discussed in this case. However, since only some of the parameter sets cause an increase in PTTL to be followed by a decrease, it is desirable to attempt to understand why. To this end, the data of figure 3.3 was separated into two groups, those that provide the decrease and those that do not. These data were then normalized for ease in viewing and are shown in figures 3.4 and 3.5, respectively.

First consider the effects of the electron traps. From figure 3.4, one finds that decreasing the concentration or trapping probability of trap 1, or increasing the concentration or trapping probability of trap 2, produces an increase followed by a decrease. However, from figure 3.5, we see that making the opposite changes, increasing the concentration or trapping probability of trap 1, or decreasing the concentration or trapping probability of trap 2, does not produce the decrease in PTTL. The changes that produce a decrease are those that cause more electrons to be trapped in trap 2. The other changes do just the opposite, namely, trap more electrons in trap 1. This seems to imply that in order to observe the decrease in the PTTL signal, fewer electrons must be trapped in trap 1 at the start of the heating phase.

Considering the recombination centers, we find that changing the concentration or hole trapping probabilities for either recombination center will have little effect on the shape of the PTTL verses illumination time curve. In all cases, the PTTL increases then decreases. This is similar to the results from the simple model. In the simple model, there was little change in the shape or magnitude of the curve. Here, the shape does not change much but the magnitude does. This is simply due to the fact that here we have two

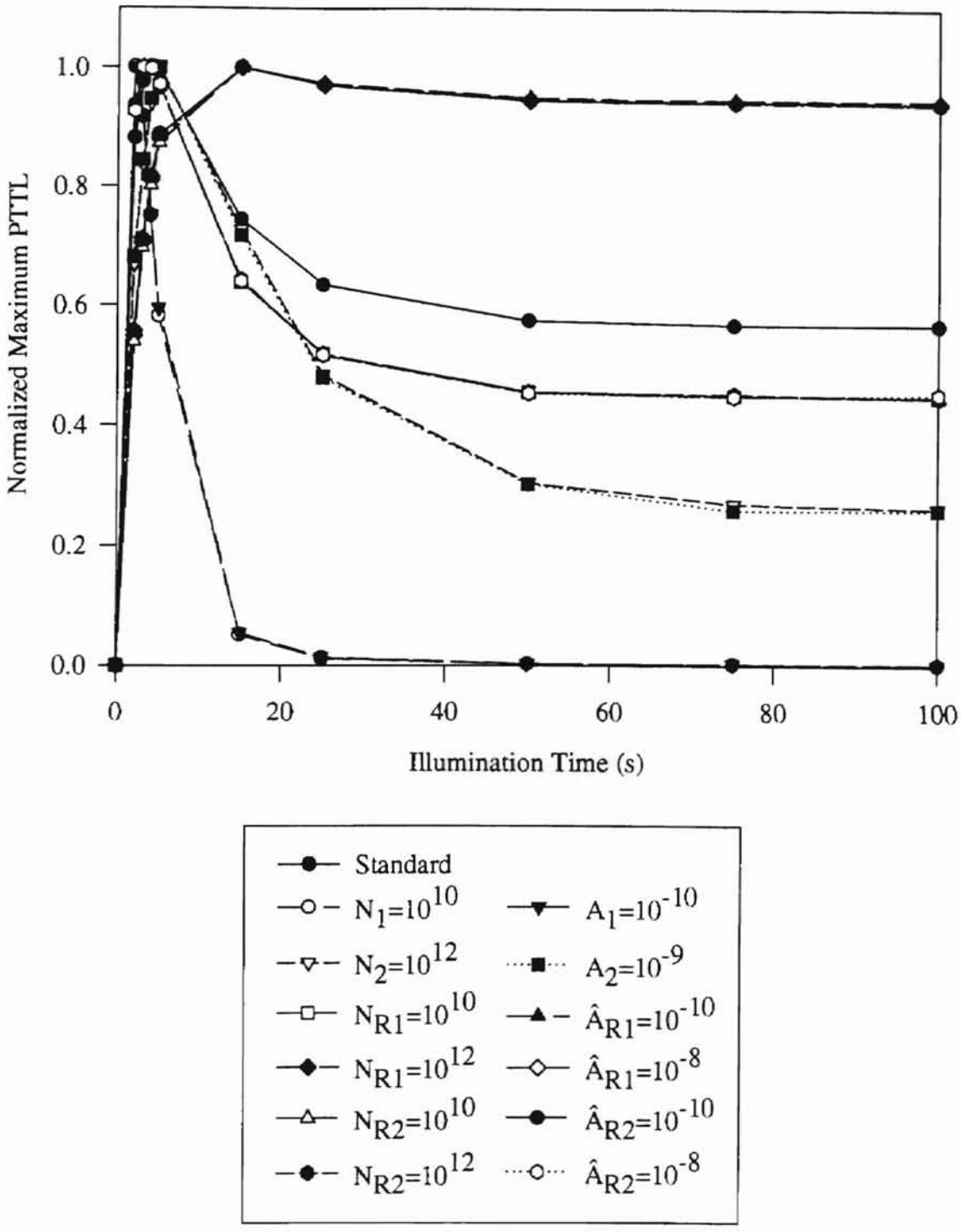

Figure 3.4: Numerically simulated PTTL time response for the model of figure 2.4. Each curve represents a change in the parameter indicated. These changes produced curves with an initial increase followed by a decrease.

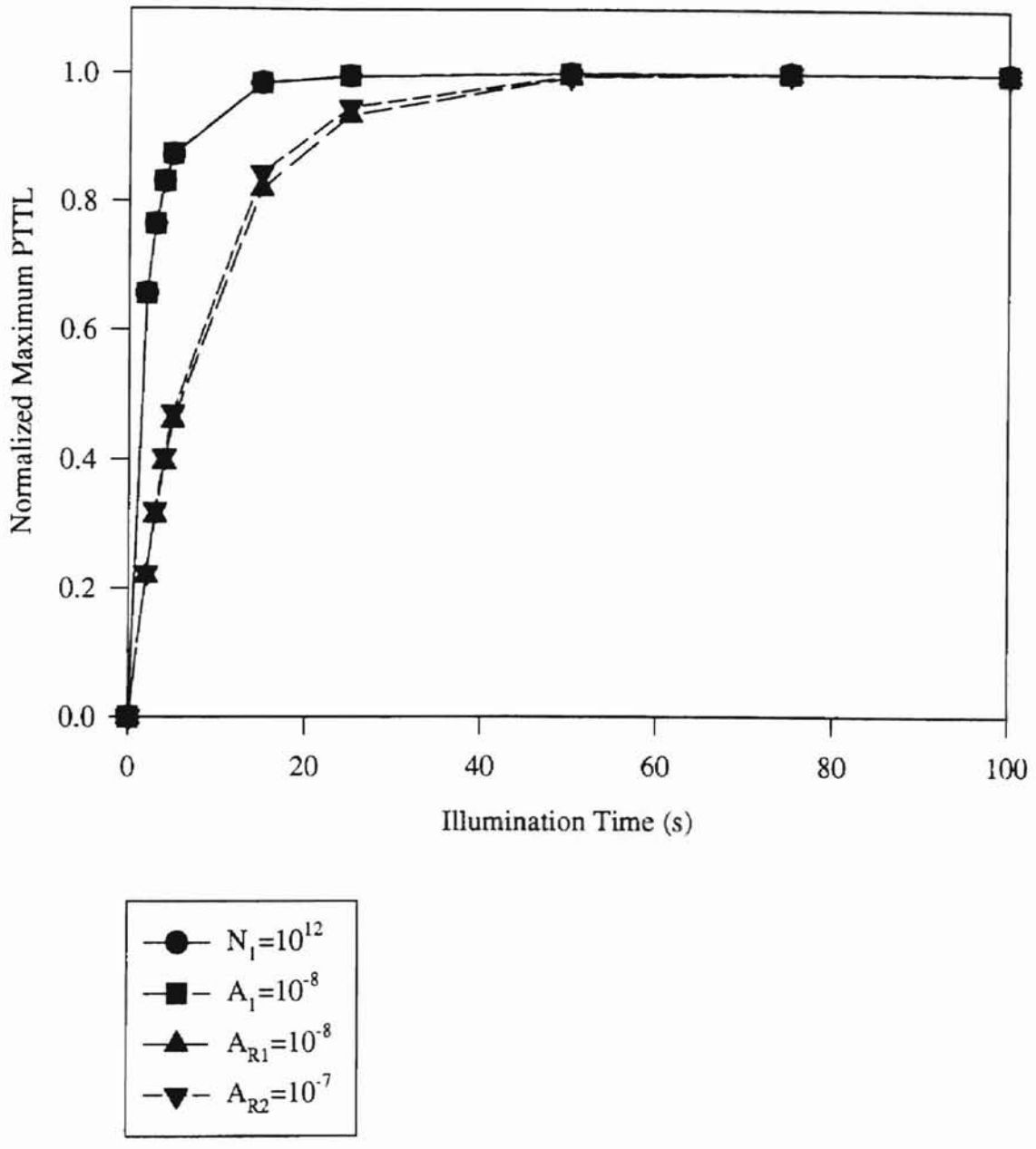

Figure 3.5: Numerically simulated PTTL time response for the model of figure 2.4. Each curve represents a change in the parameter indicated. These changes produced curves that monotonically increase to a steady state value.

recombination centers. There will still always be an available hole for an electron to recombine with, however, changing the concentrations or hole trapping probabilities for the recombination centers causes more of these recombinations to occur at one or the other recombination center. If more recombinations occur at the luminescent recombination center, there will be a greater PTTL signal. Likewise, if more recombinations occur at the non-luminescent recombination center, then there will be a smaller PTTL signal. This is exactly what is observed.

The only recombination center parameters that affect whether or not a decrease will be observed in the PTTL signal are the recombination probabilities. From figures 3.4 and 3.5 we see that decreasing the recombination probability for recombination center R1 or increasing the recombination probability for recombination center R2 will cause no decrease to be seen. Both of these changes cause recombination to be more likely at R2 and less likely at R1. Thus, during the pre-heating and illumination phases, more recombinations will occur at R2 and more holes will remain trapped in R1. This seems to imply that there must not be too many holes trapped in R1 just before heating if there is to be a decrease in the PTTL versus illumination time.

Making the opposite changes, namely, increasing the recombination probability for recombination center R1 or decreasing the recombination probability for recombination center R2 will cause there to be no observable PTTL signal. This can be attributed to the higher likelihood of recombination occurring at R1. If all of the holes trapped at R1 during irradiation are used up prior to heating by recombinations during the pre-heating and illumination phases, then only holes at R2 will be available during the final heating.

Since recombinations at R2 do not produce observable light emissions, no PTTL will be observed.

In general, the data from this model seems to imply that in order to see an increase in the PTTL signal followed by a decrease there must be fewer electrons in trap 1 or fewer holes in R1 at the start of the heating phase. This is consistent with the theory of McKeever (1994) that the decrease is caused by removal of holes in luminescent recombination centers by recombination during illumination.

Wavelength Dependence of the PTTL Signal

The more complex model discussed above has been shown to accurately predict experimental PTTL results at a fixed optical excitation rate (equivalent to a fixed wavelength) for certain sets of model parameters. In order to test the model further, a set of simulations was conducted to determine the effect of using different wavelengths of light for optical stimulation.

Different wavelengths of light can be simulated by changing the optical excitation rate in a prescribed fashion. Recall that the optical excitation rate is equal to $f\sigma$. The photoionization cross section, the only wavelength dependent parameter describing the PTTL process, is, for deep traps, given by

$$\sigma(h\nu) = C\sqrt{E_o}\,\frac{(h\nu - E_o)^{3/2}}{h\nu(h\nu - \gamma E_o)^2} \tag{3.1}$$

where h is Plank's constant, E_o is the optical ionization energy of the donor trap, ν is the frequency of the light ($\lambda = c / \nu$), and C and γ are constants (Böer, 1990). For quartz, C = 8.39×10^{-16} eV cm^2 and $\gamma = 0.559$ (Morris, 1995). Thus, to simulate different stimulation wavelengths, $\sigma(\lambda)$ was calculated using equation 3.1 and then multiplied by a photon flux, f. The photon flux served only to alter the time constant of the excitation and was adjusted to give a time response similar to that seen experimentally.

Using the same procedure as before, several simulations were conducted. In each simulation, the wavelength of the stimulation light was varied by the method described above. It was assumed that the optical ionization energy of trap 2, E_o in equation 3.1, was 2.25 eV. The maximum PTTL signal was plotted verses the time of illumination for each wavelength. The results are shown in figure 3.6. From the figure one can see that regardless of the stimulation wavelength, the obtained PTTL maximum is a constant value. It will be shown that the experimental results, to be presented in the following chapter, do not exhibit this behavior. However, the shape of the curves is similar to that seen experimentally in some cases.

Experimental evidence, to be presented later, will show that over the wavelength range of 300 nm - 500 nm, there is more than one trap from which electrons are being optically excited in quartz. In an attempt to model this, a third trap was added to the model. This new model is shown in figure 3.7. The parameters of the new trap, trap 3, were assumed to be identical to those of trap 2, except that trap 3 was assumed to have an optical ionization energy of 3.10 eV, compared with 2.25 eV for trap 2. Thus, electrons in both traps will be optically excited by light with wavelength less than 400 nm. Above 400 nm, only electrons in trap 2 will be optically excited. These optical ionization

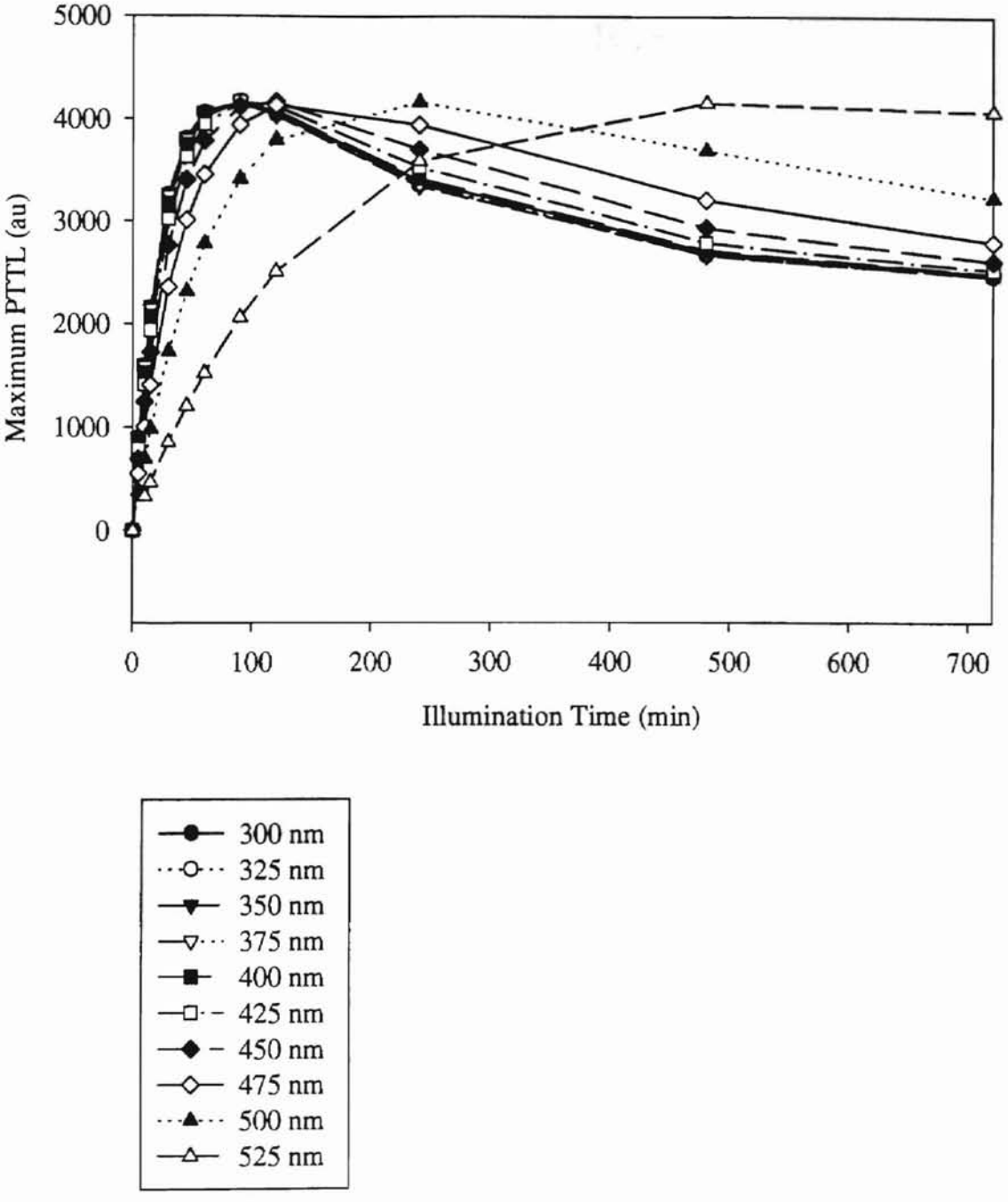

Figure 3.6: Numerically simulated PTTL time response for the model of figure 2.4. Each curve represents a different stimulation light wavelength.

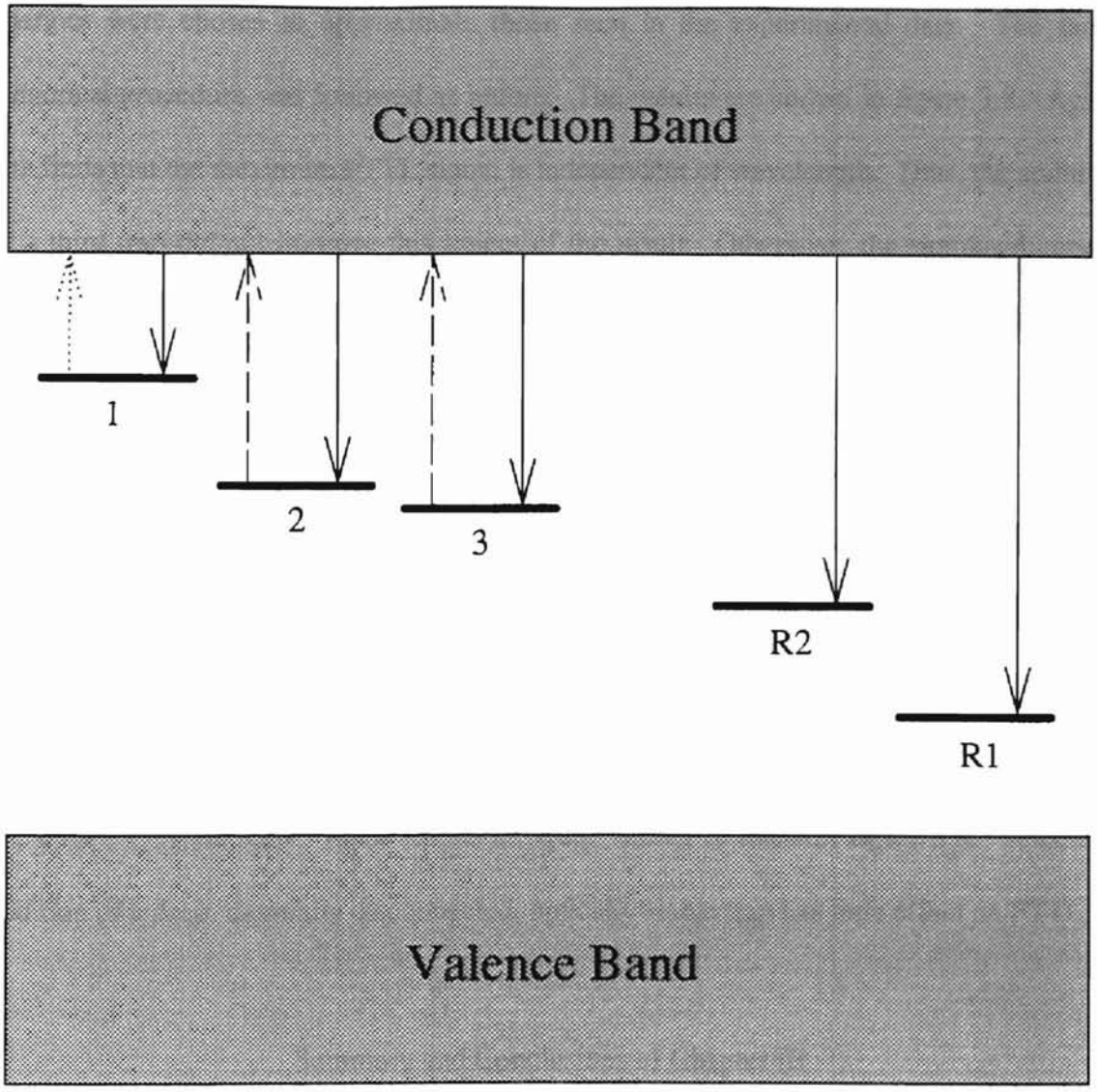

Figure 3.7: Schematic diagram of the band structure for the more complex PTTL model with a third trap added. Each level is described in the text. Thermal excitation is indicated by a dotted line. Optical excitation is indicated by a dashed line. Trapping and recombination is indicated by a solid line.

energies were chosen to approximate those seen in the experimental data. The same numerical procedure was followed as before. The results are shown in figure 3.8. Again one finds that the maximum PTTL signal is independent of wavelength. Thus, the addition of a third trap did not improve this aspect of the result. Otherwise, the simulated curves are quite similar to experimental results. Further discussion of this comparison follows the experimental data.

One last attempt was made to remove the constant maximum behavior from the model. A fourth trap was added to the model. This trap was assumed to be very deep and thus thermally disconnected. Also, no electrons were allowed to be optically excited from this trap. Thus, the trap serves only as another source of competition for electrons. This model is shown in figure 3.9. The same procedure was followed as before. The results are shown in figure 3.10. These results are quite similar to those of figure 3.8. Thus, the addition of a deep, thermally disconnected, optically stable trap has little effect on PTTL.

Summary and Conclusions of Chapter III

The two models introduced in chapter II have been numerically solved. The sensitivity of these models to the various parameters has been determined. The time response of the PTTL signal in several models was determined. The wavelength dependence of the more complex model and two additional models were presented. Comparison to experimental results was performed.

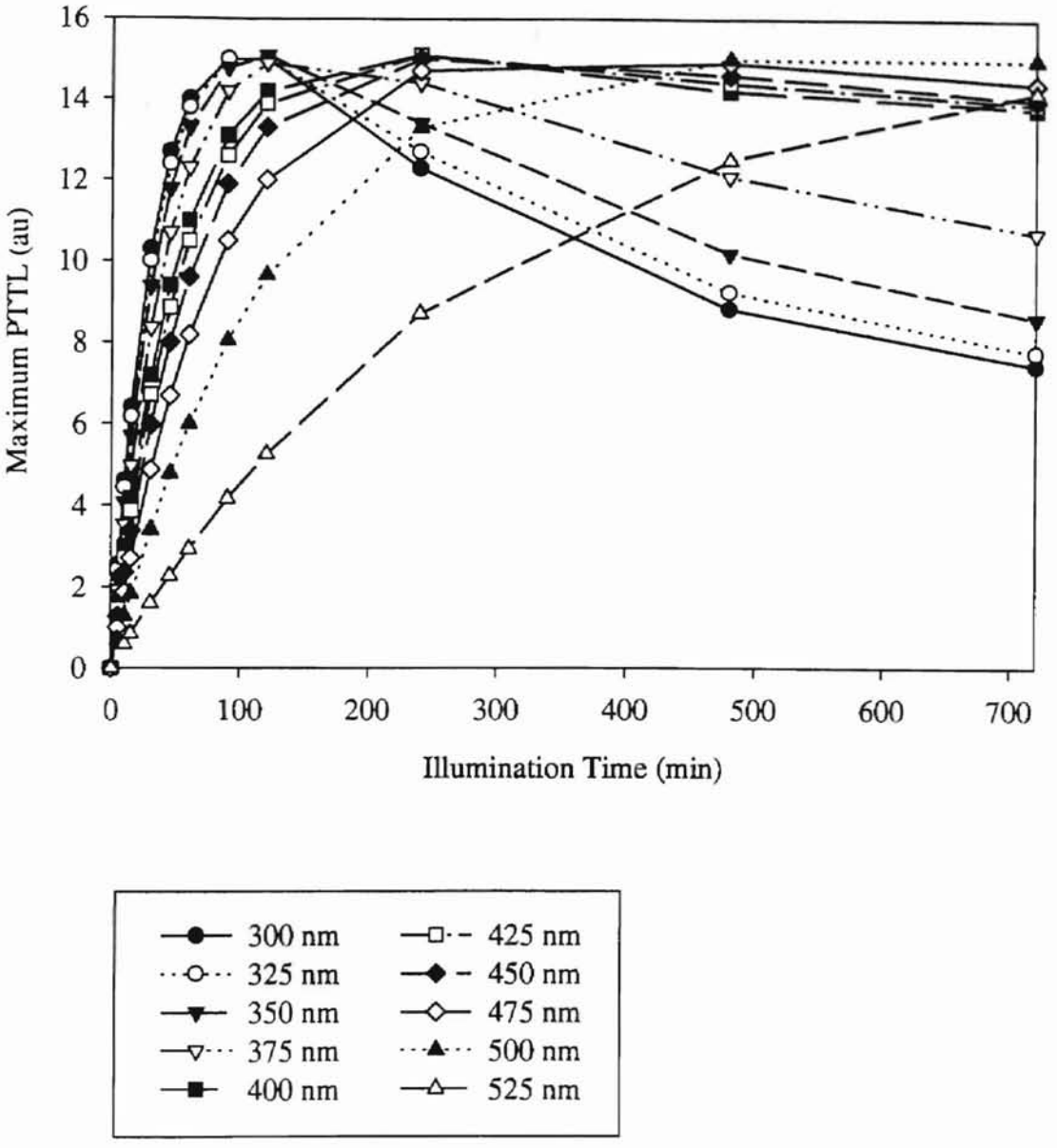

Figure 3.8: Numerically simulated PTTL time response for the model of figure 3.7. Each curve represents a different stimulation light wavelength.

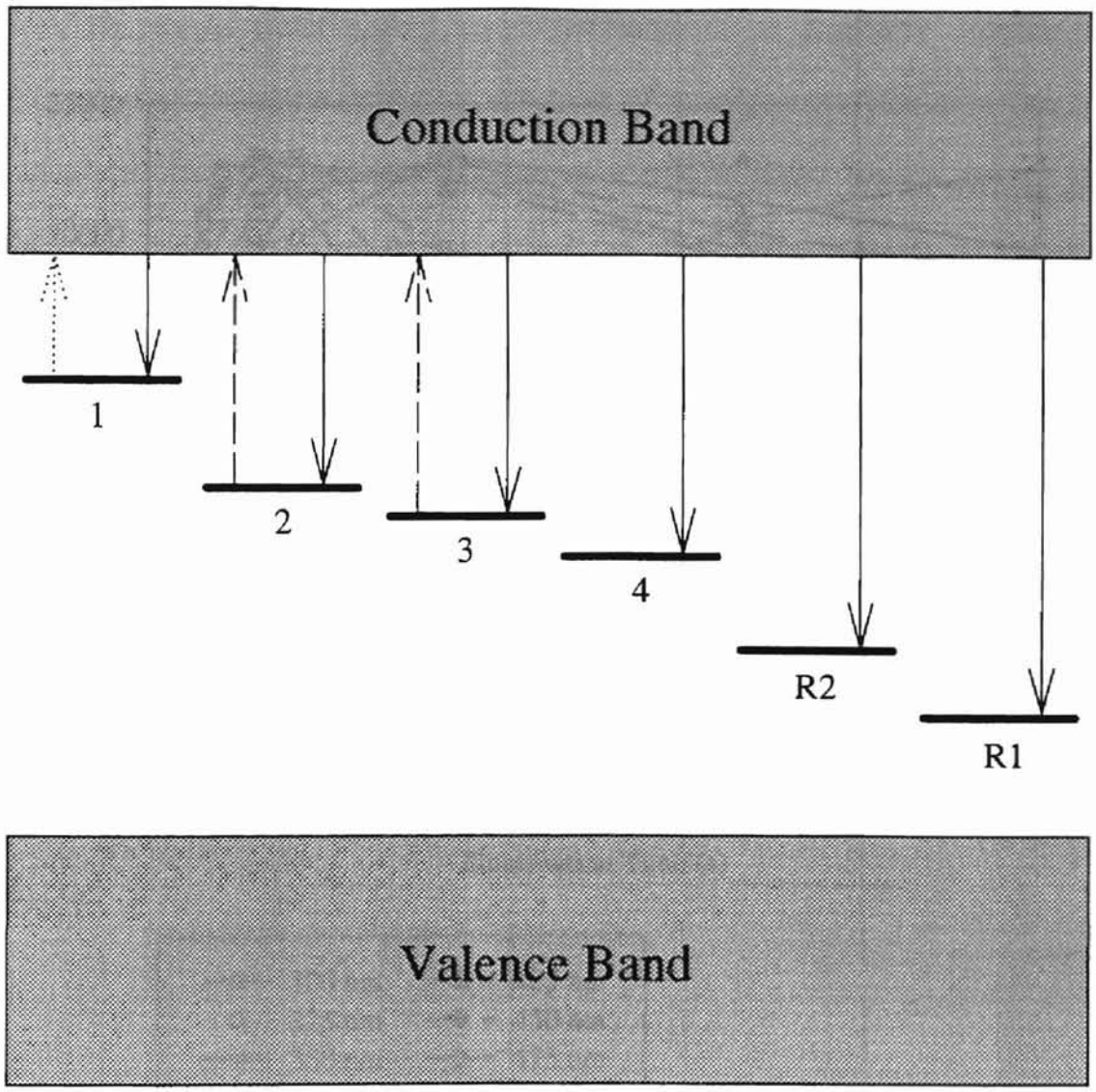

Figure 3.9: Schematic diagram of the band structure for the more complex PTTL model with two traps added (3 and 4). Each level is described in the text. Thermal excitation is indicated by a dotted line. Optical excitation is indicated by a dashed line. Trapping and recombination is indicated by a solid line.

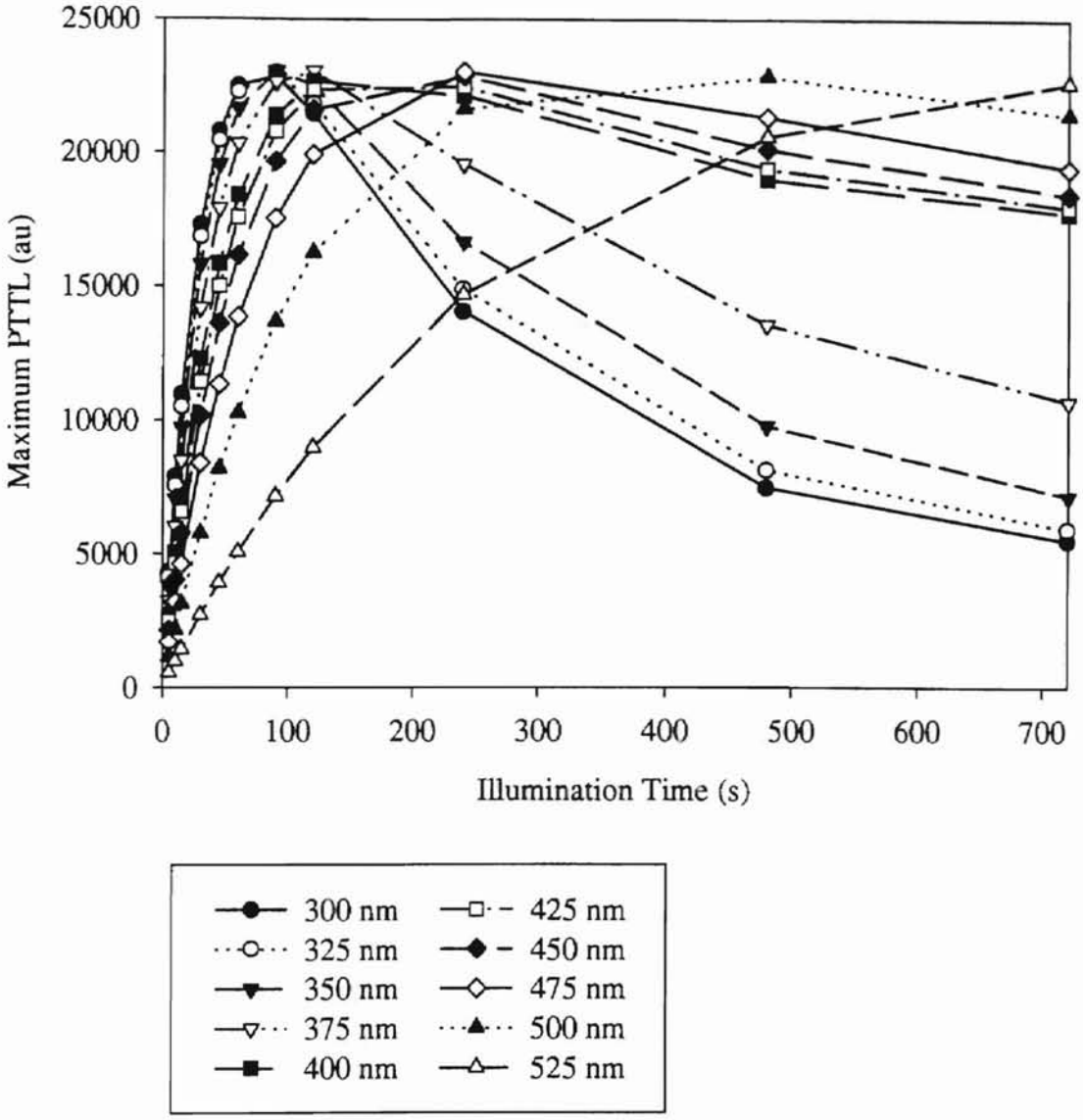

Figure 3.10: Numerically simulated time response for the model of figure 3.9. Each curve represents a different stimulation light wavelength.

The simple model proved to be too simplistic to accurately describe the experimentally witnessed results. The simulated PTTL responses of the more complex models were found to be similar to those seen experimentally, but not exact. The discrepancy between the simulated data and the experimental data can not be fully explained at this time.

In general, the results support the model of McKeever (1991). The addition of a second non-luminescent recombination center to the simple model was essential. The addition of further traps is needed to simulate experimental results. Additional deep traps have little effect on the PTTL.

CHAPTER IV

EXPERIMENTAL RESULTS

Several experiments were conducted in order to determine the experimental illumination time response of the PTTL signal in both natural and synthetic quartz. These experiments will be described in this chapter, including sample preparation procedures and experimental conditions. The results will then be presented along with proposed methods for analyzing the results.

Experimental Details

Sample Preparation

The samples used in these experiments were different types of fine powdered quartz. The basic sample preparation procedure was to select a grain size fraction of powdered quartz, then anneal, irradiate, and pre-heat the powder. All of the powders were prepared using the same procedure.

Initially the desired type of quartz was ground into a powder using an agate mortar and pestle. The resulting powder was separated by dry sieving into several grain size fractions. The grinding and separation procedures were completed by M. F. Morris. For these experiments, a grain size fraction of less than 90 μm was used.

Bøtter-Jensen *et al.* (1995) have shown that PTTL sensitivity in quartz can be significantly enhanced by high temperature annealing prior to irradiation. Due to limitations in the optical stimulation power, to be discussed later, enhancement of the PTTL signal is desirable. Therefore, the quartz powder was annealed at 950° C for one hour. This was followed by a slow cool to room temperature in the furnace. The sample was then stored in a light tight canister to prevent unwanted bleaching of the sample from this point forward.

The sample was irradiated using a ^{60}Co gamma source. The sample was exposed to the source for 120 minutes. The source delivered a dose rate of 87.6 rad / minutes Thus, the sample received a 105 Gy dose. The sample was allowed to rest in the dark at room temperature for eight hours following the irradiation to come to equilibrium.

During irradiation, charge was accumulated in the trap responsible for the 395 K TL peak (hereafter referred to as the '395 K trap'). This trap is not stable at room temperature, with a half-life of a few days. Since the experiments using each sample were conducted over several weeks, this unstable charge was removed by pre-heating the sample to a set temperature for a certain time. Stokes (1992) has noted that pre-heats that involved lower temperatures and longer durations were less prone to errors caused by a lack of reproducibility of the exact conditions. With this in mind, a series of experiments were conducted to determine the optimum pre-heat temperature and duration.

Samples of annealed, but unirradiated, powdered quartz were separated into 7.0±0.2 mg aliquots. Each aliquot was individually irradiated, then subjected to a pre-heat with the exception of one sample which was not pre-heated. The samples were then

heated to observe the TL. Optimum pre-heat conditions will remove all of the charge (thus reducing the TL to zero) from the 395 K trap while removing the least amount of charge from the higher temperature traps (e.g. 480 K). Figure 4.1 shows the results of this experiment. From the figure, one can see that both 413 K for 10 minutes and 403 K for 60 minutes removed the charge from the 395 K trap without unnecessarily removing charge from the 480 K trap. However, considering the results of Stokes, the 403 K for 60 minutes procedure was chosen in these experiments. Thus, following irradiation, all samples were pre-heated at 403 K for 60 minutes to remove the unwanted charge. This was done in darkness to prevent bleaching of the samples. After pre-heating the samples, they were cooled to room temperature and again stored in a light-tight container and stored for later use.

Experimental Procedures

In order to determine the response of the PTTL to the illumination time and wavelength, several measurements were taken. Each measurement was made using a separate aliquot taken from a single source of prepared powder. The source powder was separated into 7.0±0.2 mg samples. This sample size produced a sufficient PTTL signal while being small enough to not require a large amount of powder to be produced and stored. Each sample was placed in a small circular aluminum dish approximately 5 mm in diameter and 3 mm deep. This procedure, and all that follow, were completed in a darkened room illuminated only with red light. This prevents any charge from being

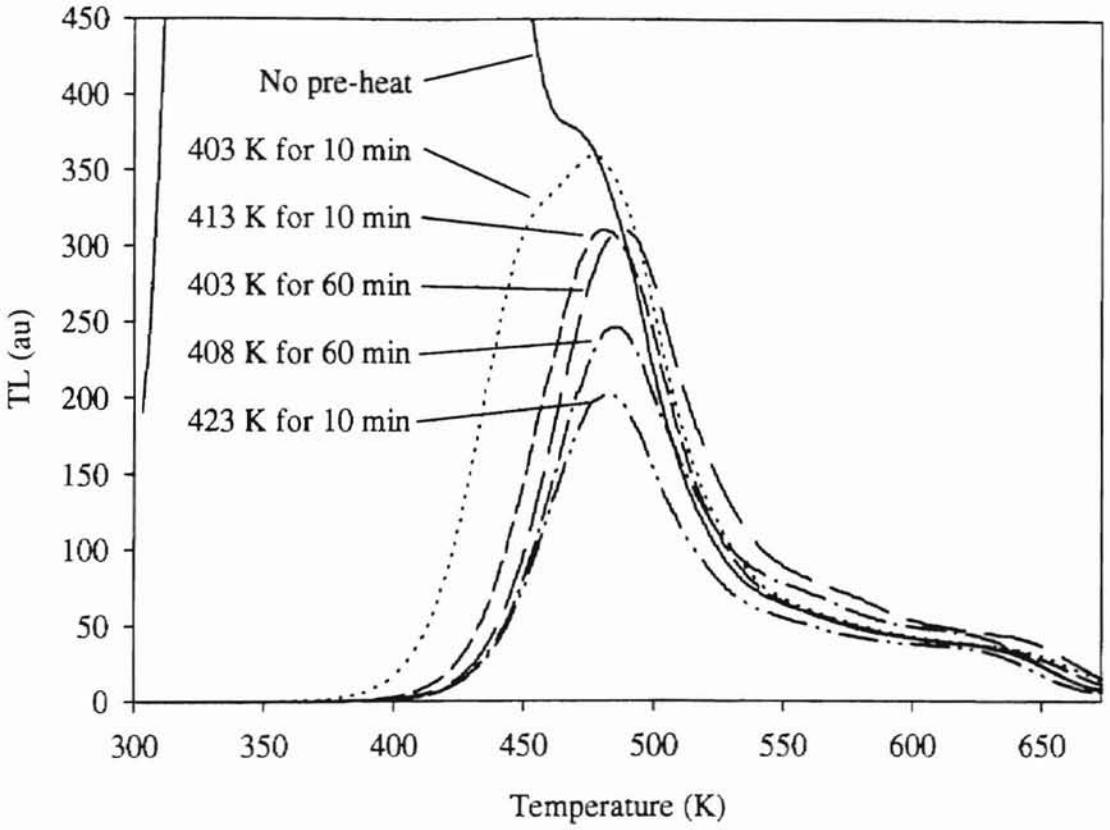

Figure 4.1: Arkansas quartz TL glow curves. Different curves represent different pre-heat treatments.

photostimulated prior to the intended illumination since the samples tested are not effected by red light.

For each measurement, a single aliquot was placed in a custom built apparatus to be illuminated and subsequently heated (see figure 4.2). The sample was placed on a small metal strip directly connected to heating and cooling control electronics. A small amount of silicone vacuum grease was used to ensure good thermal contact between the sample dish and the metal strip. In this apparatus, the sample temperature can be varied from 80 - 500 K.

After irradiation at room temperature, the sample was cooled to the illumination temperature of 100±5 K in a 10^{-4} torr N_2 atmosphere. The sample was then illuminated with monochromatic light for the desired length of time. The light source used was an Oriel 150 W Xe arc lamp. The light from the lamp was focused onto the entrance slit of a GCA McPherson monochromator with a 1200 lines/mm grating blazed at 300 nm with a dispersion of 2.65 nm/mm. Wavelengths from 300 - 500 nm were used. The light output from the monochromator was adjusted by varying the exit slit width to provide a constant photon flux of 3.19×10^{13} photons/cm^2/s at the sample at each wavelength selected. The exit slit width was varied from 1.00 - 2.00 mm. The resulting bandwidths were from 2.65 - 5.30 nm. The light was directed along a silica fiber to the sample. Adjustment of the light intensity was done by measuring the power of the light output from the silica fiber with a Newport power meter and a silicon photodiode (Newport model 818-UV). The photon flux used was selected by determining the maximum flux possible with the

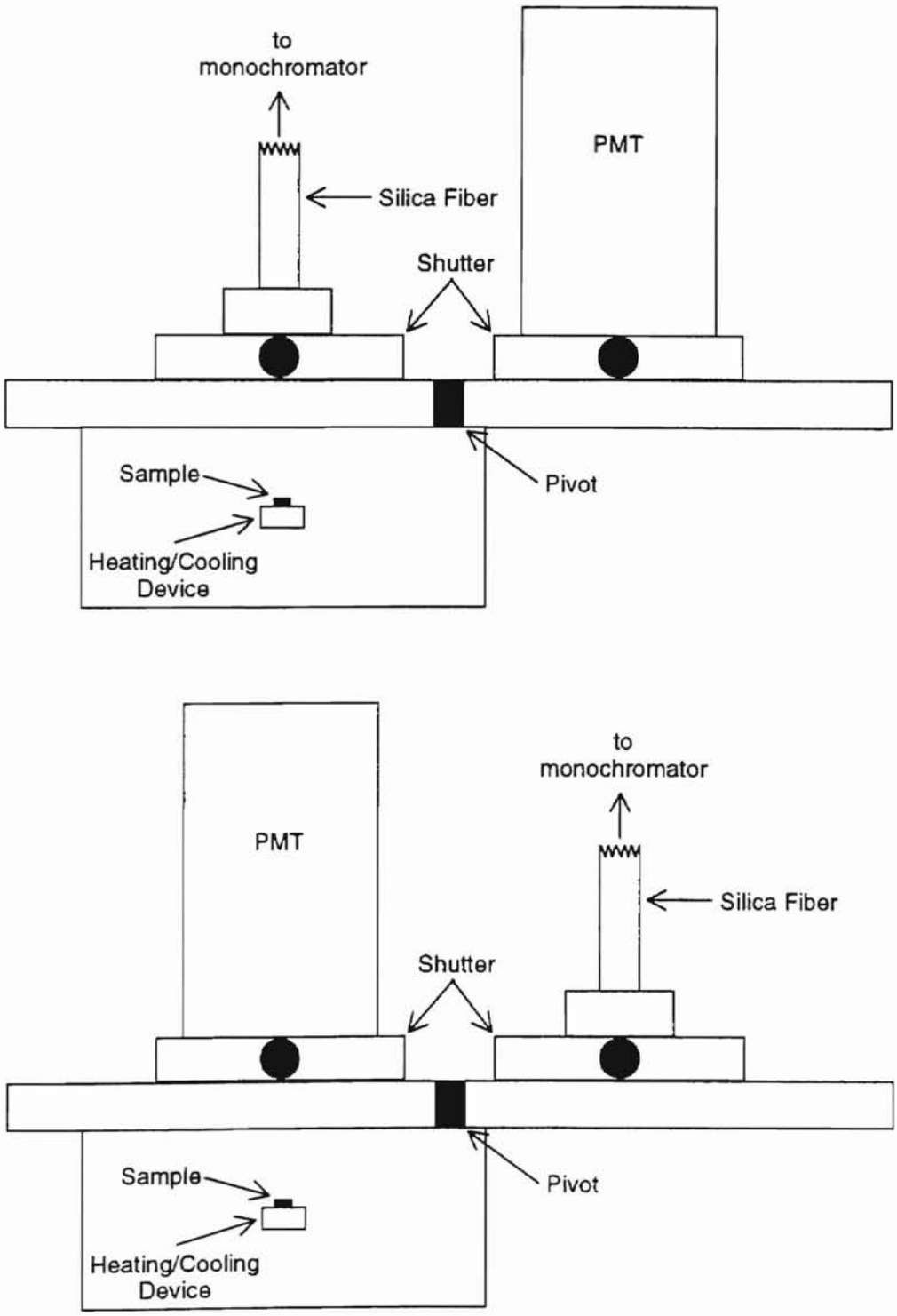

Figure 4.2: Schematic diagram of the custom illumination and heating chamber. The top figure shows the arrangement used for illumination. The bottom figure shows the arrangement used for heating and PTTL detection.

aforementioned equipment at the shortest wavelength desired (300 nm). With this photon flux, data was taken for illumination times ranging from 5 - 1440 minutes.

Following the illumination, the sample was heated to observe the PTTL signal. While the sample was being heated, nitrogen gas was introduced into the sample chamber to assist in heat conduction through the powdered sample. When heated in a vacuum, the temperature of the powder lags behind the controlled temperature of the copper mounting strip. It was determined that a 500 torr N_2 atmosphere would minimize this temperature lag. The sample was heated linearly from 100 K to 500 K at a rate of 0.91 K/s.

PTTL was produced as the sample was heated. The PTTL signal was detected using a photomultiplier tube (Thorn EMI type #9635QB) connected to a Keithley picoammeter. Both the temperature controller and the picoammeter were connected to an IBM compatible XT computer via an IEEE 488 GPIB interface. Data was collected using custom written software.

Results

A series of experiments was conducted on a sample of natural Arkansas quartz. Figure 4.3 shows a typical PTTL signal, or *glow curve*. From the figure, one sees several glow peaks which are labeled according to the temperature at which they occur.

All of the peaks, except the 480 K peak, are not present in samples which have not been illuminated. Figure 4.4 shows a TL glow curve for an unilluminated sample as well as the data of figure 4.3. One can see that the height of the 480 K has been reduced in the illuminated sample. The reason for this behavior can be understood by considering the

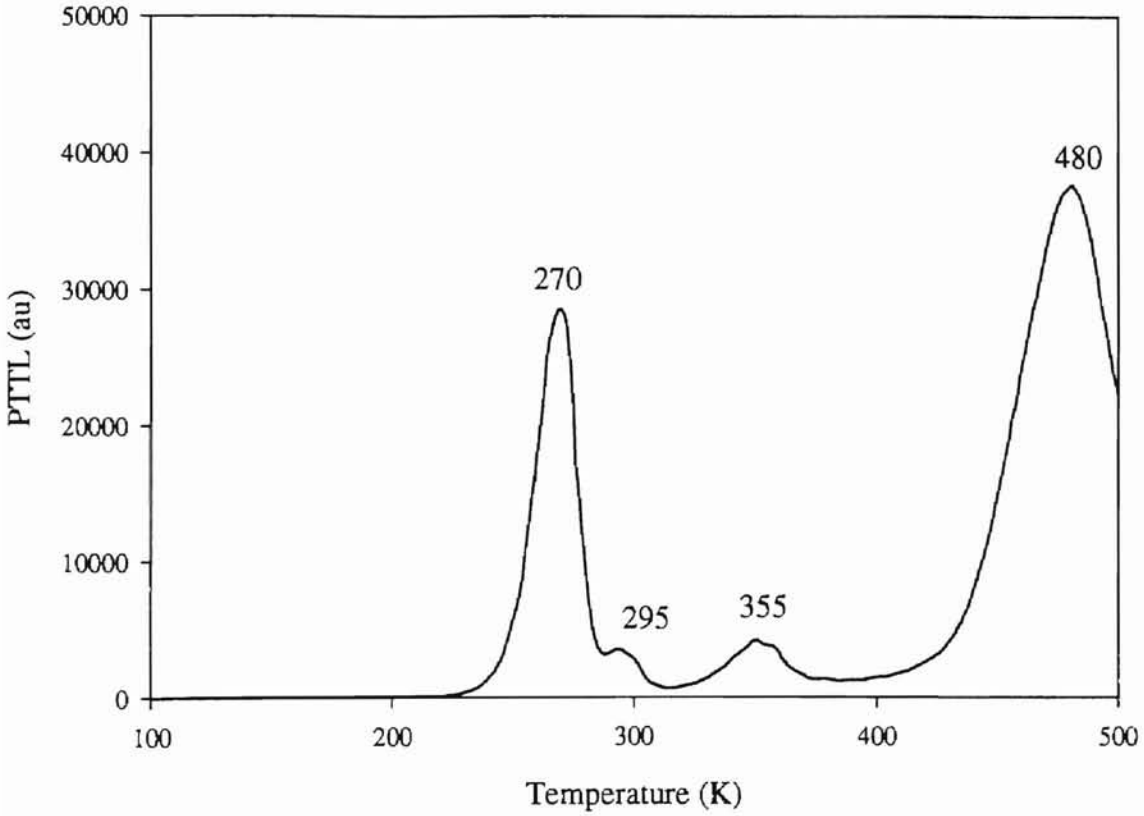

Figure 4.3: Arkansas quartz PTTL glow curve following a 60 minute exposure to 350 nm light. The most prominent peaks are labeled according to the temperature at which they occur.

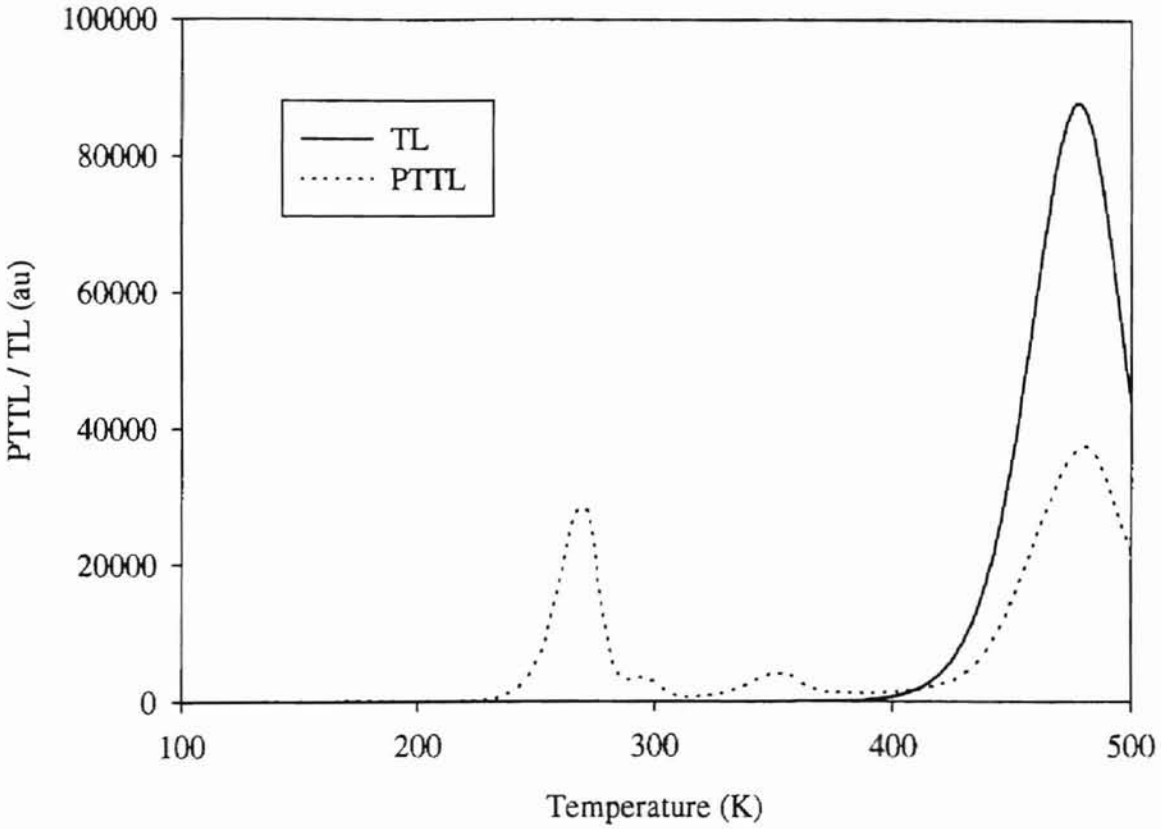

Figure 4.4: Arkansas quartz TL and PTTL glow curves. PTTL is that of figure 4.3.

trapped charge. The heights of the glow peaks are proportional to the charge trapped in an electron trap. Each peak represents a different trap. Recall that as the sample is illuminated, charge is phototransferred from deep traps (e.g. the 480 K trap) to shallow traps (e.g. the 270 K, 355 K, etc. traps). Thus, the charge in the deep traps is reduced and charge is accumulated in the shallow traps. This explains the reduction in the size of the 480 K peak and the increase in the other peaks following illumination.

Figure 4.5 shows a family of PTTL glow curves resulting from illuminations at a fixed wavelength (350 nm) for varying lengths of time. From the figure, one can see that the heights of the glow peaks change with the illumination time. For some peaks (e.g. 255 K, 270 K, 295 K) the PTTL is seen to increase up to some maximum then decrease. Similar results have been observed by Jain (1984) and Milanovich-Reichhalter and Vana (1990, 1991). This behavior can best be illustrated by plotting the peak height as a function of illumination time. This is done in figure 4.6.

Note that in all cases, the PTTL signal does not decrease to zero, but rather reaches a non-zero steady state value. Even after 24 hours of illumination (see figure 4.7) the PTTL had not been reduced to zero. No appreciable change was observed in the PTTL beyond about 12 hours. These results imply that the traps which cause these peaks must not be loosing charge due to optical excitation during illumination. If charge was being optically removed from these traps, then, given a long enough illumination period, all of the charge would be removed from the traps and would recombine. Upon heating the sample, no PTTL signal would be observed. Thus, a non-zero steady state PTTL

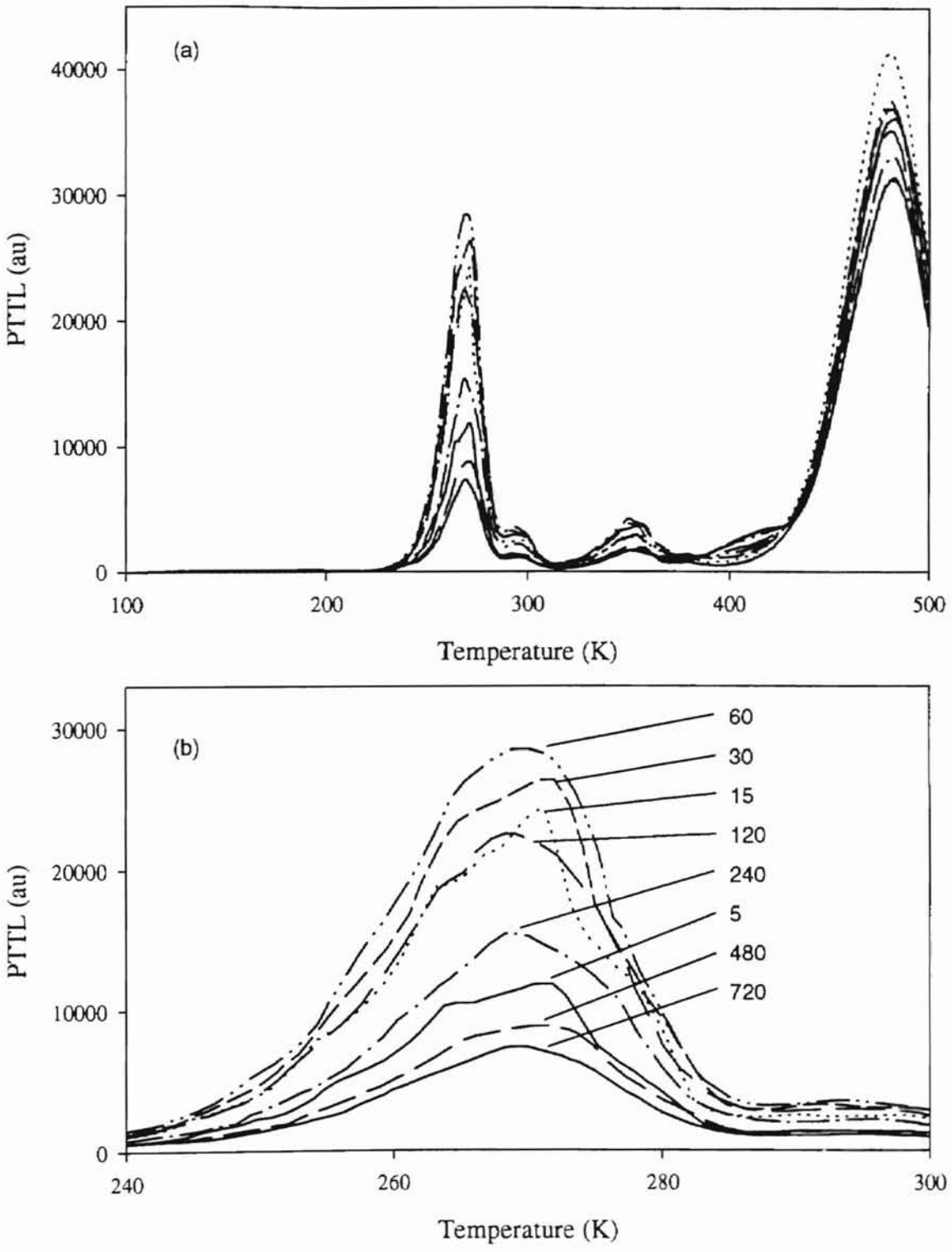

Figure 4.5: Arkansas quartz PTTL glow curves following exposure to 350 nm light for the times indicated. (a) shows the complete curves. (b) shows the data of the 270 K peak enhanced and labeled by illumination time in minutes.

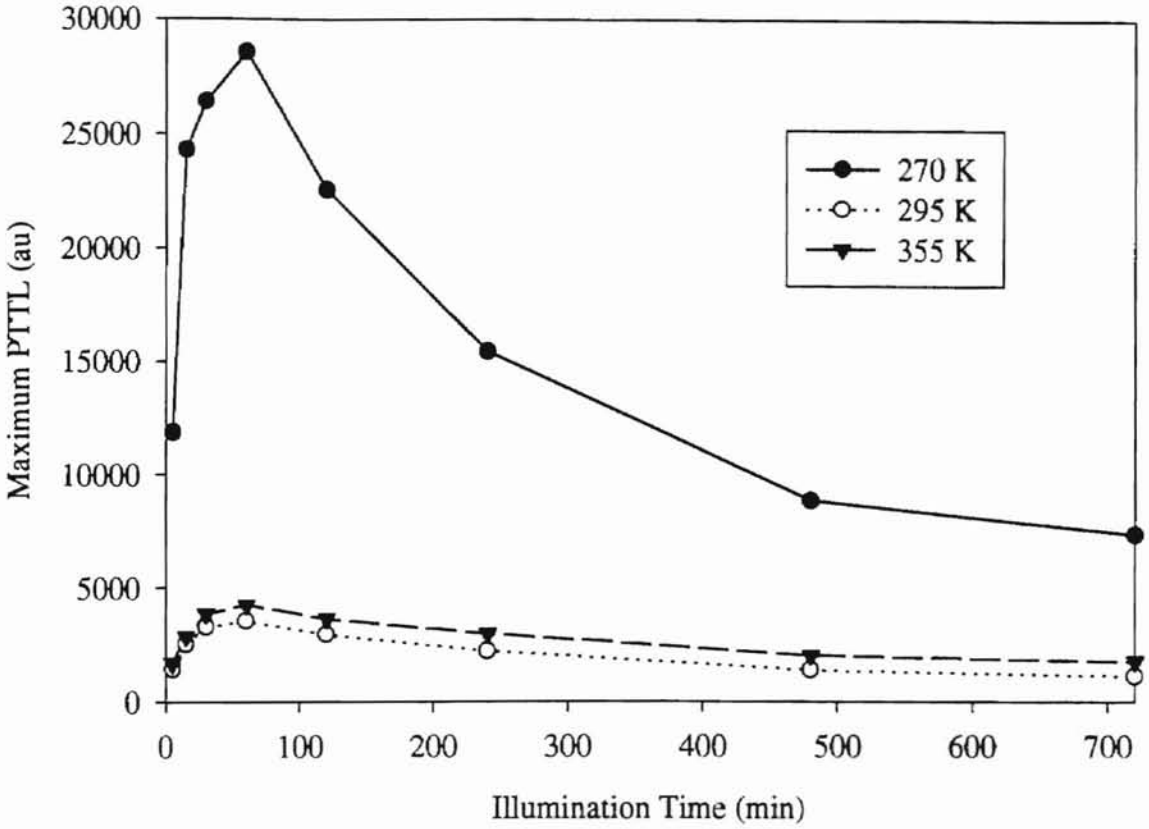

Figure 4.6: Arkansas quartz maximum PTTL time response of several prominent peaks following exposure to 350 nm light.

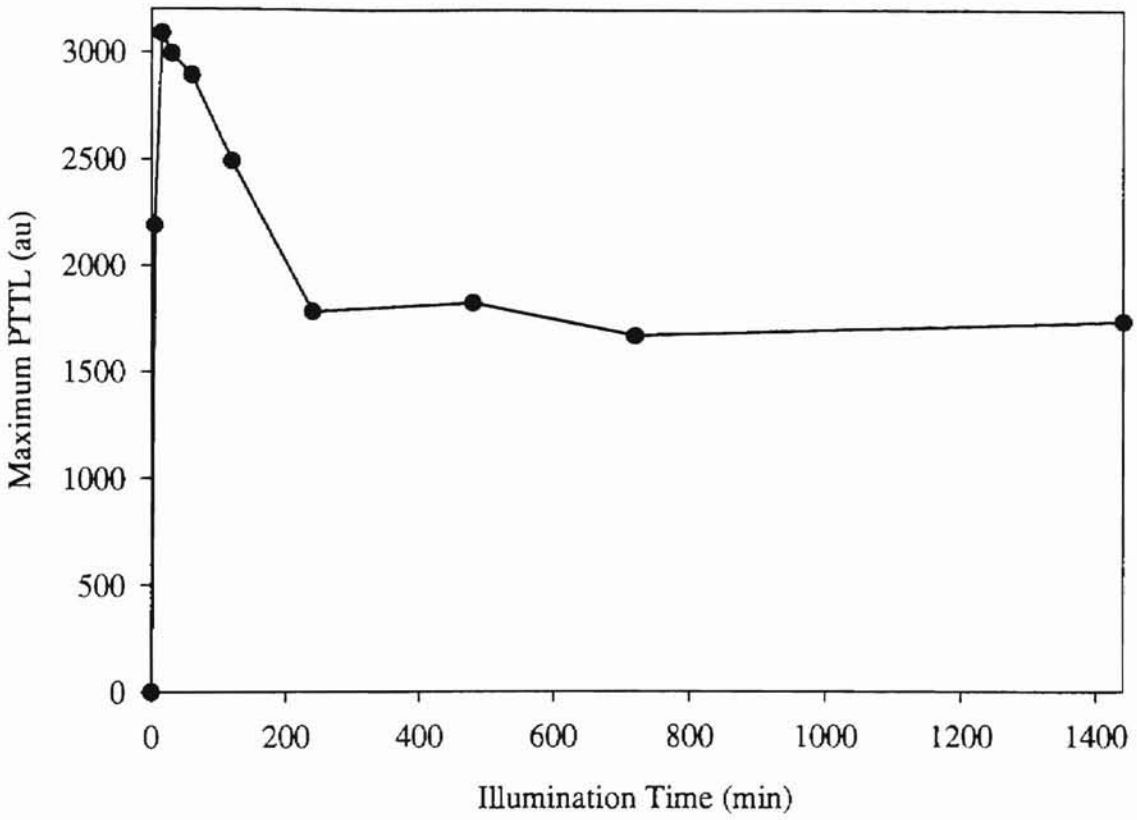

Figure 4.7: Arkansas quartz maximum PTTL time response of the 295 K peak following exposure to 325 nm light.

signal can not be explained by optical excitation of electrons out of the shallow traps. This behavior supports the theory of McKeever (1994).

The effect of stimulation wavelength on the PTTL time response was also studied. Data similar to those of figure 4.6 was taken using different wavelengths of stimulation light. The results for the 270 K peak are shown in figure 4.8. The other PTTL peaks show similar results. The data is characterized by an increase in the maximum PTTL signal with decreasing wavelength.

Recall from chapter III (see figure 3.10) that the numerically simulated data exhibit the initial increase in PTTL followed by a decrease but do not show an increase in the maximum PTTL signal with decreasing wavelength. This discrepancy can not be readily explained except to say that there is some physical wavelength dependent phenomena present in the experimental samples that is not being accurately accounted for in the model used (see figure 3.9). It is encouraging to note, however, that if the shortest wavelength data is removed from figure 4.8, as in figure 4.9, then the experimental data is quite similar to the simulated data. Thus, it is expected that the missing phenomenon is negligible at longer wavelengths but rapidly becomes more important as the wavelength is decreased below approximately 375 nm.

The wavelength response of PTTL was also considered. Historically, the wavelength response of PTTL has been determined by selecting an arbitrary, fixed illumination time and observing the PTTL produced by various wavelengths of light (Jain 1984, Milanovich-Reichhalter and Vana (1990, 1991), Morris and McKeever, 1994). The wavelength response for the Arkansas quartz sample was determined using this procedure and is shown in figure 4.10. Since, as previously discussed, the PTTL signal is believed to

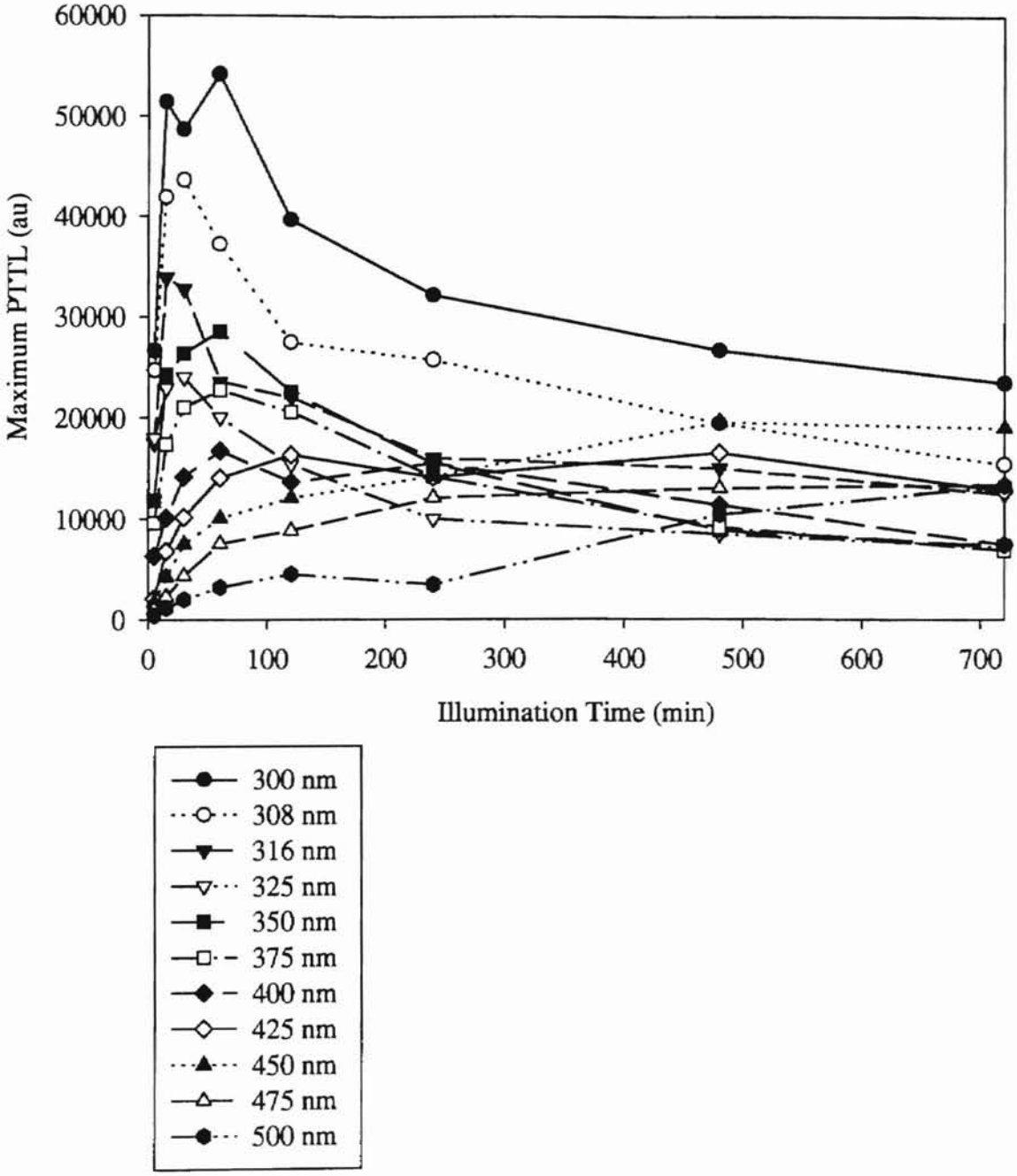

Figure 4.8: Arkansas quartz maximum PTTL time response of the 270 K peak. Data is after illumination with light of the wavelength shown.

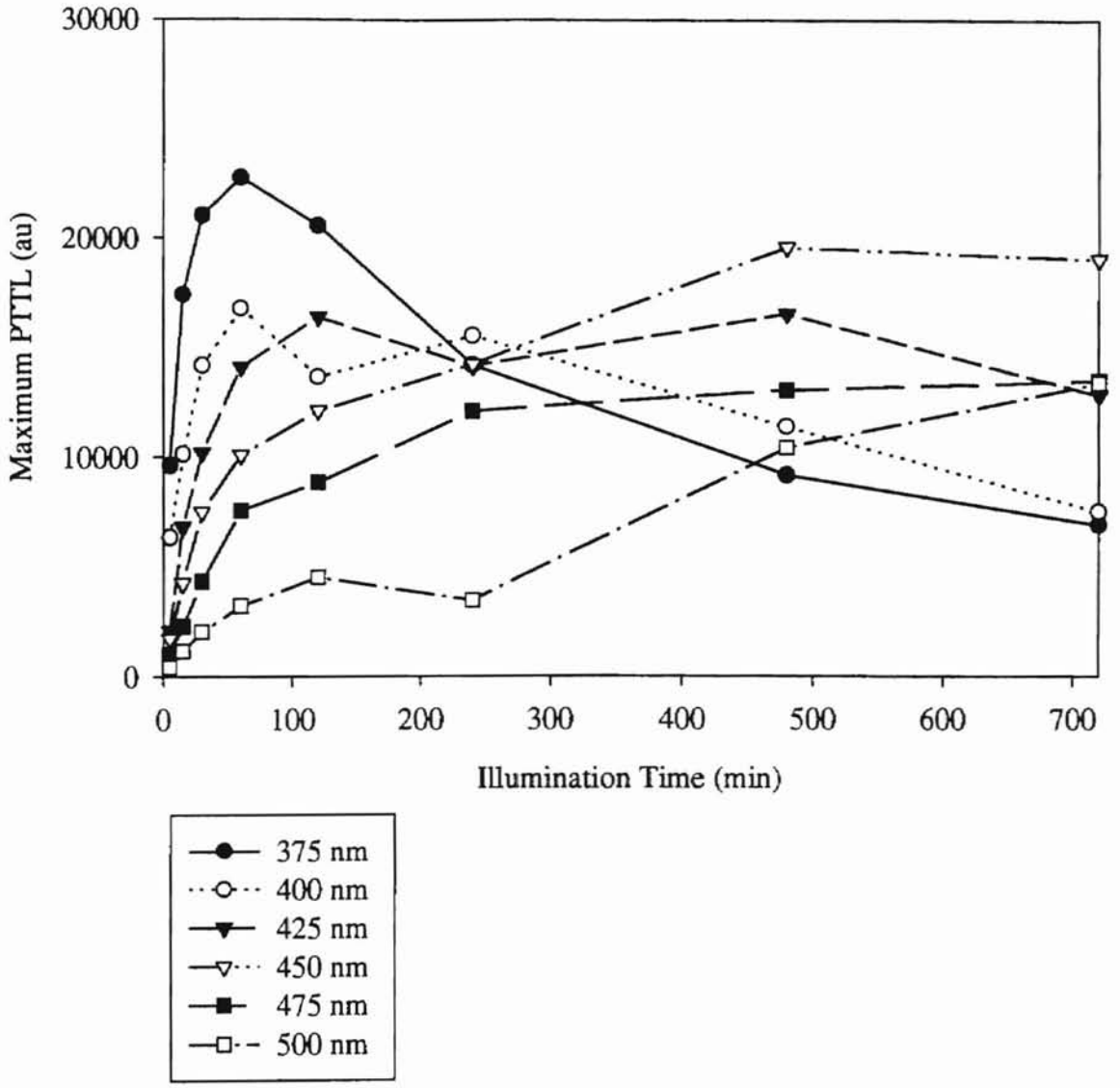

Figure 4.9: Arkansas quartz maximum PTTL time response of the 270 K peak. Data is after illumination with light of the wavelength shown. The data of figure 4.8 is repeated with the exception of the lower wavelengths used.

be caused by the transfer of charge from deep traps to shallow traps, the wavelength response for the bleaching of the TL signal from these deep traps should be identical to that for PTTL. The wavelength response for the bleaching of the 480 K and 535 K traps in Arkansas quartz was determined and is shown in figure 4.11. In the figure, the percentage of the total (unbleached) TL that is lost due to phototransfer out of these traps during illumination is plotted against the wavelength of the stimulation light used. These latter data are consistent with those previously shown by Spooner (1994) and by Morris and McKeever (1994). By comparison of figures 4.10 and 4.11, however, one finds that the wavelength response of PTTL is *not* similar to the wavelength response for the bleaching of TL in Arkansas quartz. This can be understood by considering figures 4.8 and 4.9. From the figures one sees that by varying the illumination time, the relative effects of different wavelengths can be changed. The wavelength response of PTTL determined by the historically accepted procedure is dependent on the fixed illumination time chosen. For example, figure 4.12 shows the wavelength response of PTTL determined in this manner for Arkansas quartz using 60 and 480 minutes as the fixed illumination time. Note the difference in the shapes of the two curves. Therefore, this procedure is equivocal and is not valid as a method to determine the PTTL wavelength response. With this in mind, a new procedure was developed to extract the wavelength dependence of PTTL from the experimental data.

The wavelength dependence of PTTL is derived from the photoionization cross-section. In the numerical simulations discussed earlier (see chapter III), the photoionization cross-section was varied according to equation 3.1. Thus, the shape of the wavelength dependence of PTTL is known beforehand and the goal is to extract this

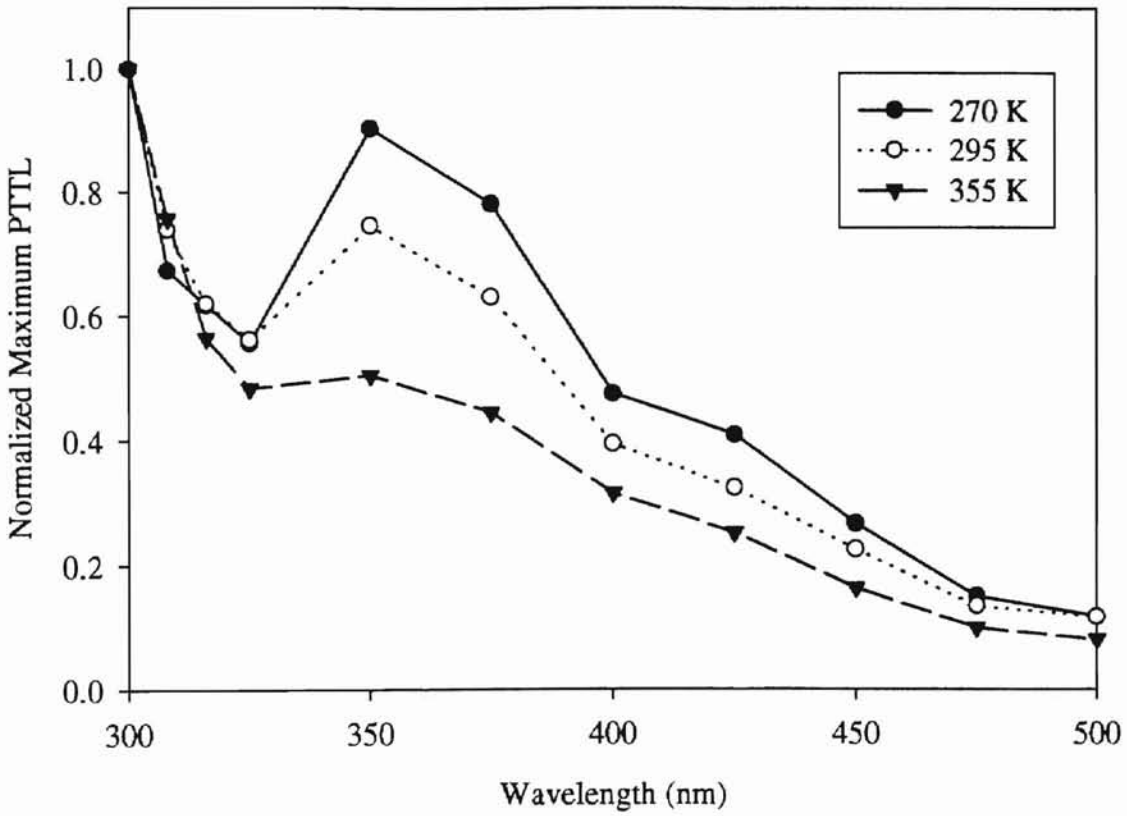

Figure 4.10: Arkansas quartz PTTL wavelength response following a 45 minute exposure. Each curve represents a different PTTL peak.

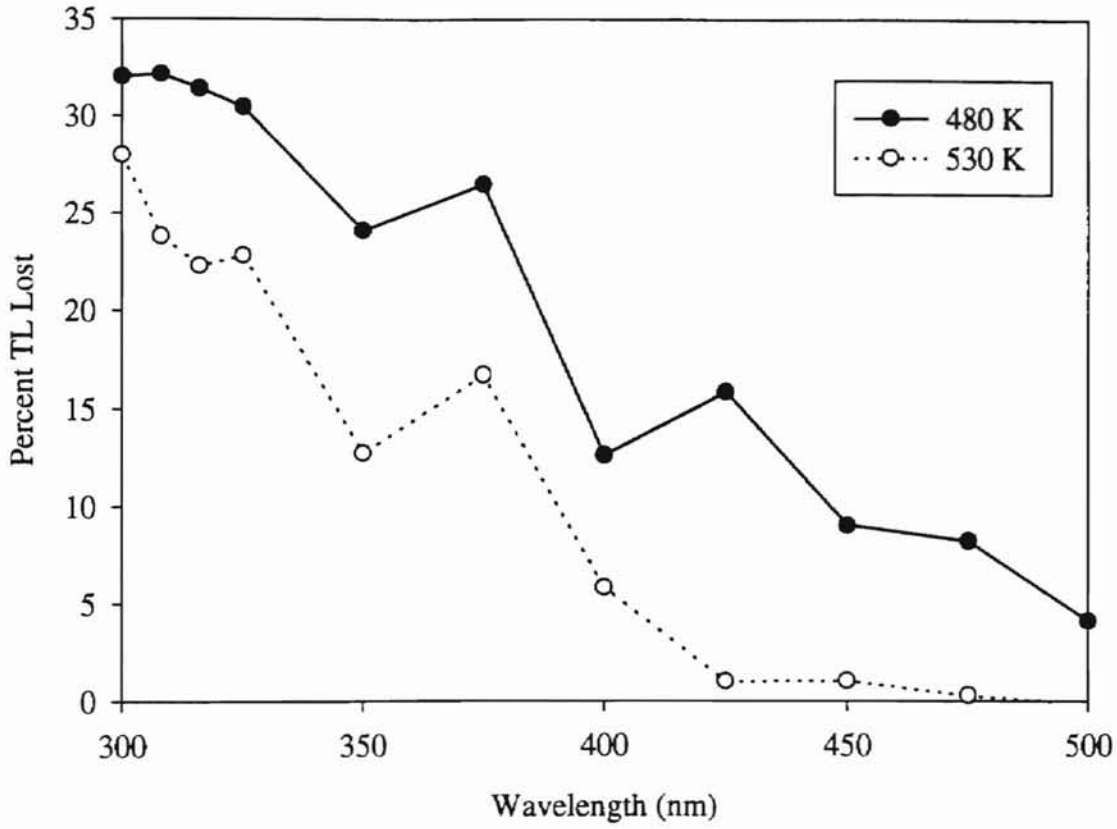

Figure 4.11: Percent TL lost from a sample of Arkansas quartz following a 45 minute exposure. Each curve represents a different TL peak.

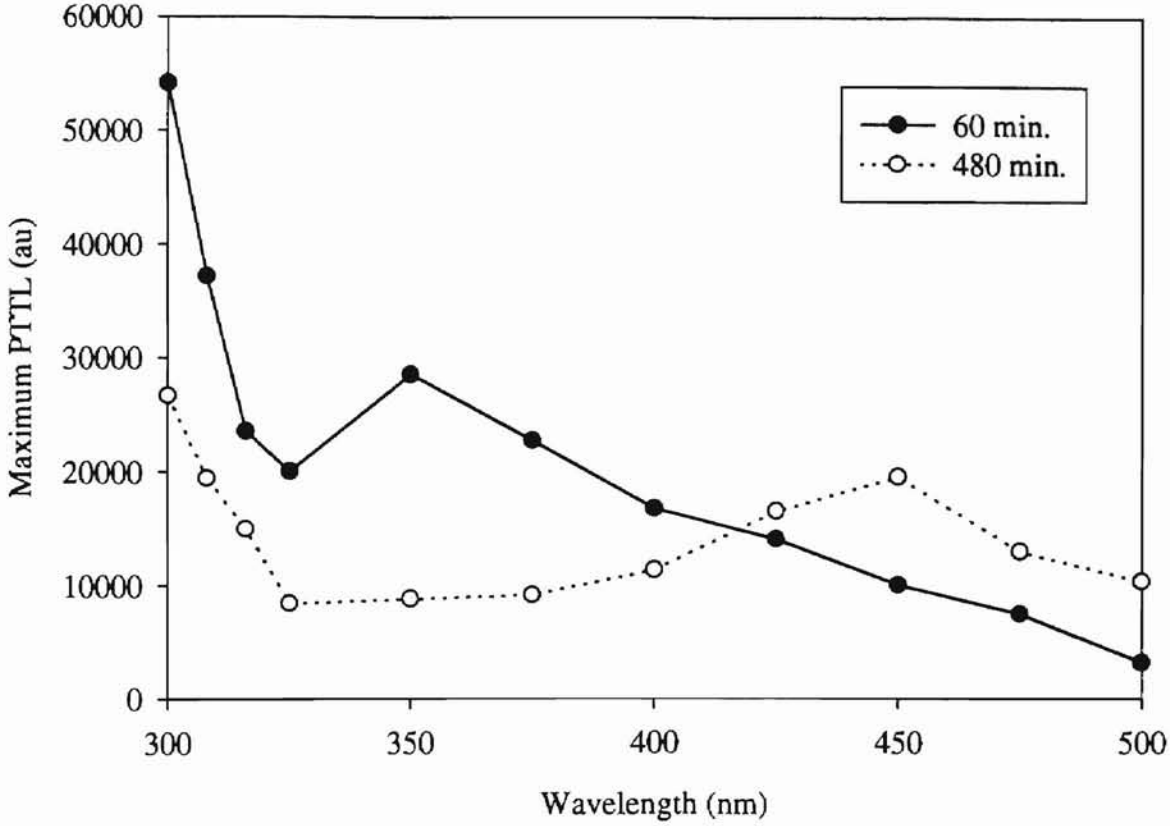

Figure 4.12: Wavelength response of PTTL for Arkansas quartz determined by the historically accepted method using the fixed illumination times shown. Note the curves are not similar, especially in the region around 350 nm.

information from the simulated PTTL data. It was found that by taking the *initial slope* of the PTTL versus illumination time curves shown in figure 3.10 and plotting this versus wavelength, the shape of the wavelength dependence of PTTL could be found. Figure 4.13 shows the wavelength dependence of PTTL obtained in this manner for the simulated data, compared with the shape of the photoionization cross-section used. Note the excellent agreement between the two curves. Thus, this method may be used to extract the PTTL wavelength response from the PTTL versus illumination time data.

Working with the experimental PTTL data for Arkansas quartz, the wavelength response was determined using the above procedure. The results are shown in figure 4.14. From the figure, it can be seen that the shape of the PTTL wavelength response is similar regardless of the PTTL trap used in the analysis. This supports the method, since each PTTL trap is being filled during illumination with electrons from the same deep traps. By comparing figures 4.14 and 4.11 one finds that the PTTL wavelength response determined in this manner is similar to the wavelength response for bleaching of TL. This provides further support for this method of extracting the wavelength dependence of PTTL from the experimental data.

Comparing figure 4.14 to figure 4.13, it appears that over the wavelength range of 300 - 500 nm there are at least two and possibly three source traps responsible for the PTTL signal in Arkansas quartz. However, in the wavelength range of green light there appears to be only one source trap being optically emptied. This is consistent with the findings of Spooner (1994), Ditlefsen and Huntley (1994), and Duller and Bøtter-Jensen (1996).

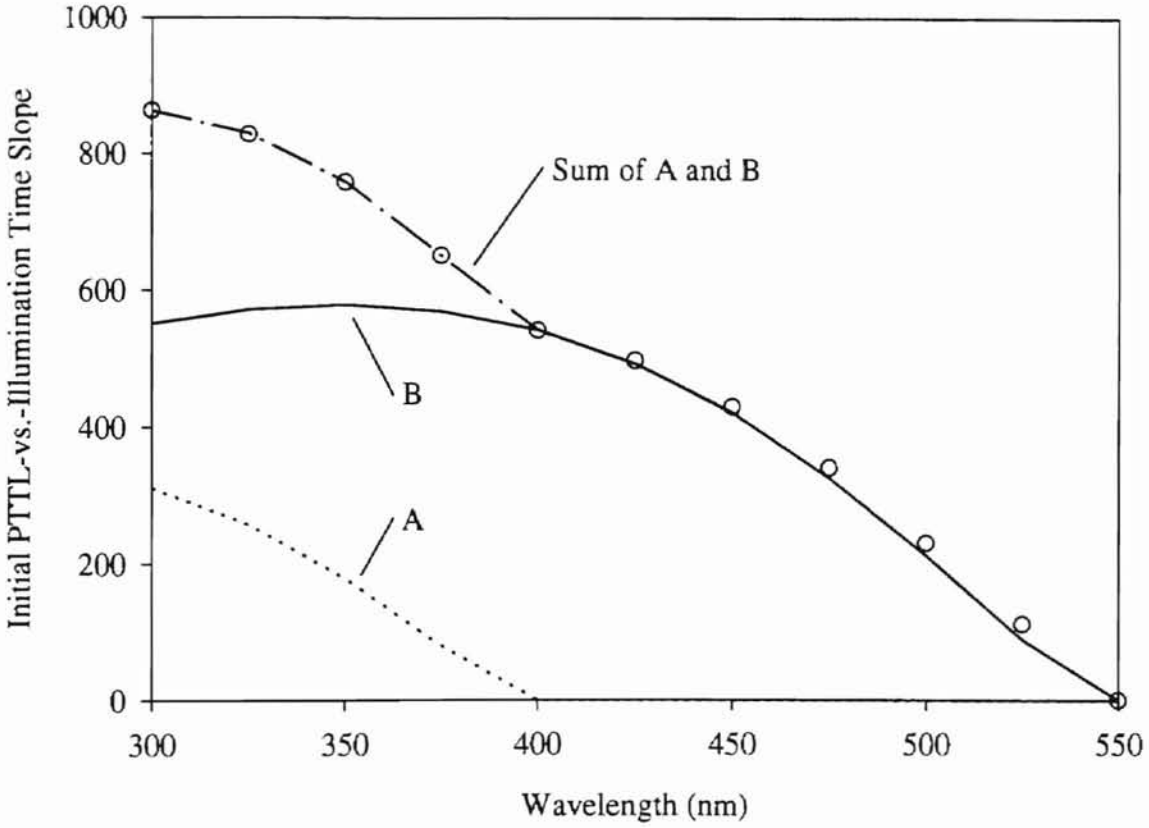

Figure 4.13: The initial slope of the numerically simulated PTTL time response curves (figure 3.10) is plotted (open circles) against stimulation wavelength. The model of figure 3.9 was used in the simulation. The photoionization cross-section of each trap is also shown (curves A and B). The cross-sections have been rescaled using the 300 nm and 400 nm data points. The sum, A+B, agrees well with the initial slope data from the numerical simulations.

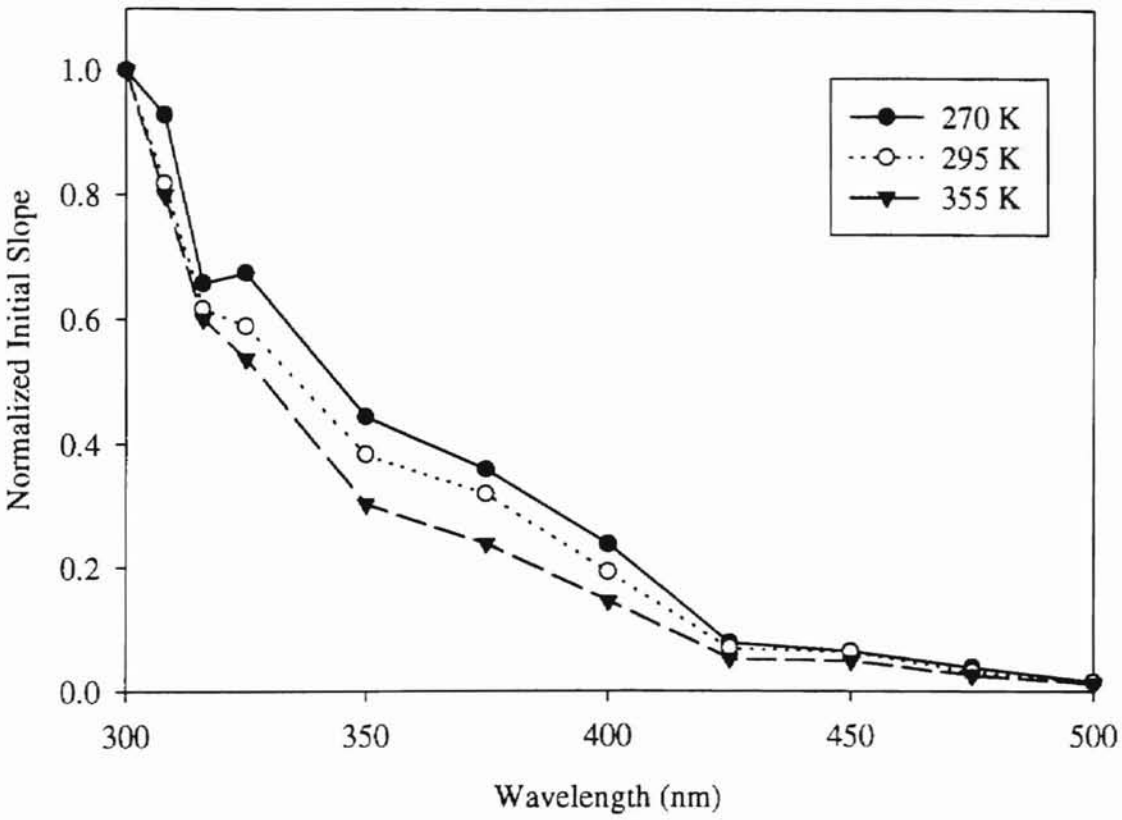

Figure 4.14: The initial slope of the maximum PTTL time response curves (refer to figure 4.8) for Arkansas quartz is plotted against the wavelength of the illumination light. Each curve represents a different PTTL peak.

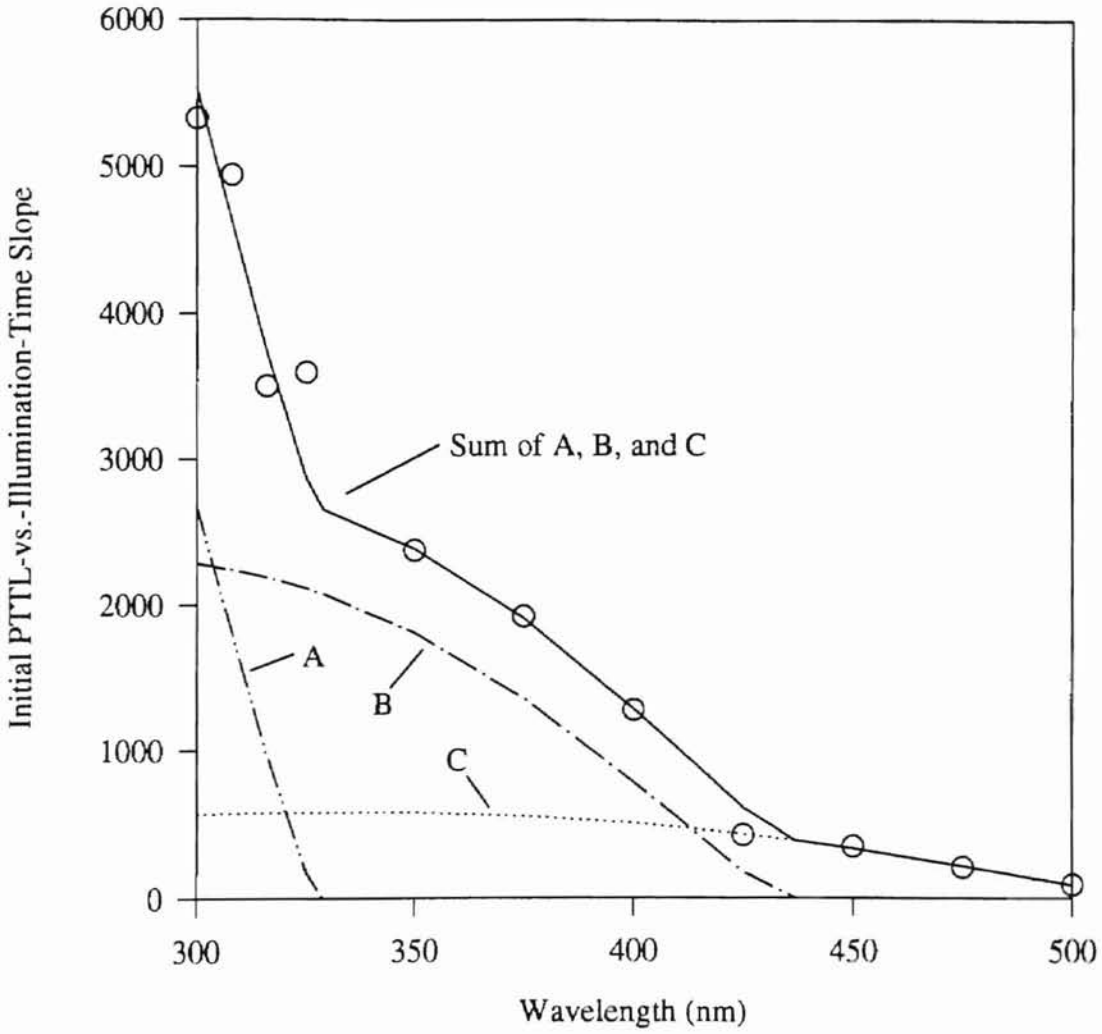

Figure 4.15: The initial slope data for the 270 K peak of figure 4.14 is shown (open circles) along with the numerical fit of equation 4.1. The three components of equation 4.1 are also shown (curves A, B, and C).

From the data of figure 4.14, the ionization energies of the deep source traps can be determined. Figure 4.15 shows an attempt to fit the data of figure 4.14 for the 270 K peak to the sum of three curves representing the photoionization cross-sections of three source traps ($\sigma(\lambda)$ from equation 3.1). That is:

$$S(\lambda) = \sum_{i=1}^{3} K_i \sigma_i(\lambda) = \sum_{i=1}^{3} C_i \sqrt{E_{oi}} \frac{(\lambda - E_{oi})^{3/2}}{\lambda(\lambda - 0.559E_{oi})^2} \qquad (4.1)$$

where $S(\lambda)$ is the normalized initial slope of the PTTL versus illumination time curve and Ki and Ci are constants. There is good agreement between the fit and the data. This further supports the claim that there are three source traps present in this wavelength range. The three optical ionization energies found were 2.37 eV, 2.84 eV, and 3.77 eV.

In addition to Arkansas quartz, Premium-Q single crystal synthetic quartz was also studied. Figure 4.16 shows a typical PTTL glow curve. By comparing figures 4.3 and 4.16, one can see that there is considerable variation in the size and number of glow peaks present in the two samples.

The time response of the PTTL signal was determined for the synthetic quartz. Figure 4.17 shows the time response as a function of wavelength. Note that these results are similar to those for the Arkansas quartz samples. The time response again shows an increase in PTTL followed, in some cases, by a decrease as well as a non-zero steady state value of PTTL at long bleaching times. Also, after removal of the lowest wavelength data, there is some agreement between the experimental data and the simulated data of figure 3.10.

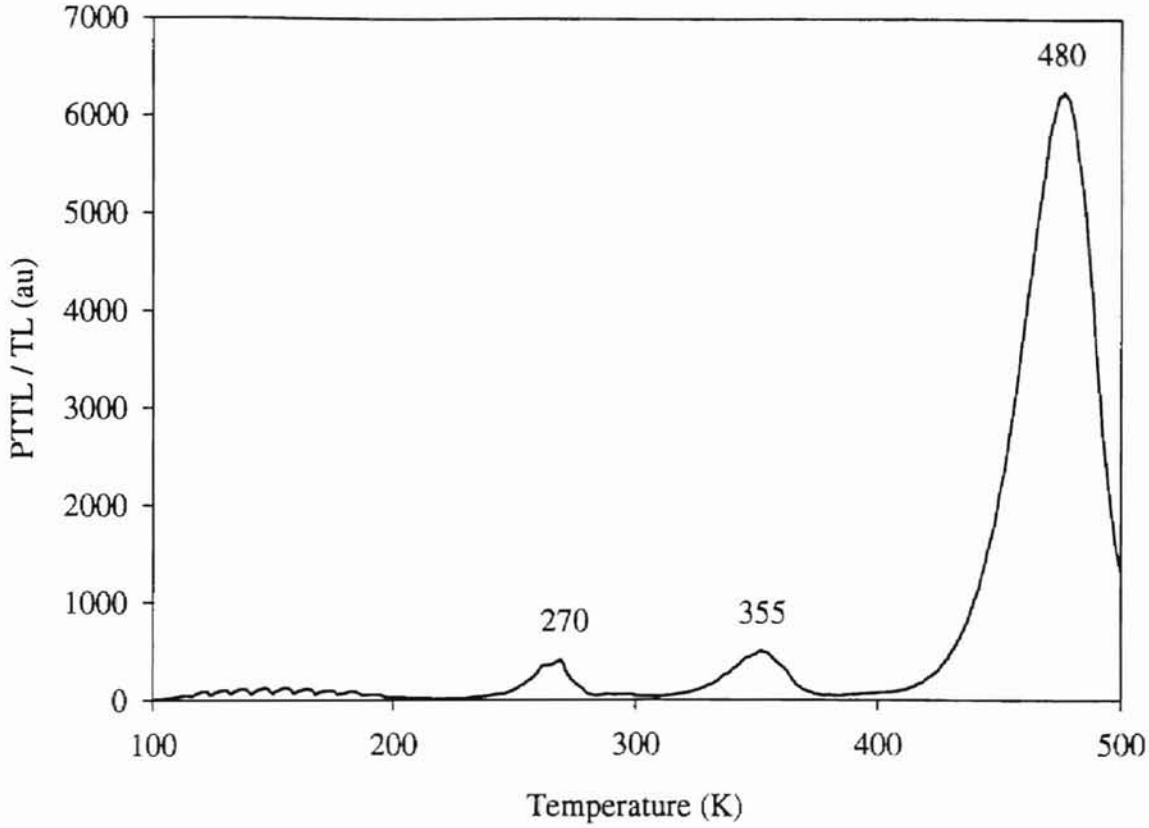

Figure 4.16: Premium-Q quartz PTTL glow curve following exposure to 350 nm light for 60 minutes. The most prominent peaks are labeled according to the temperature at which they occur.

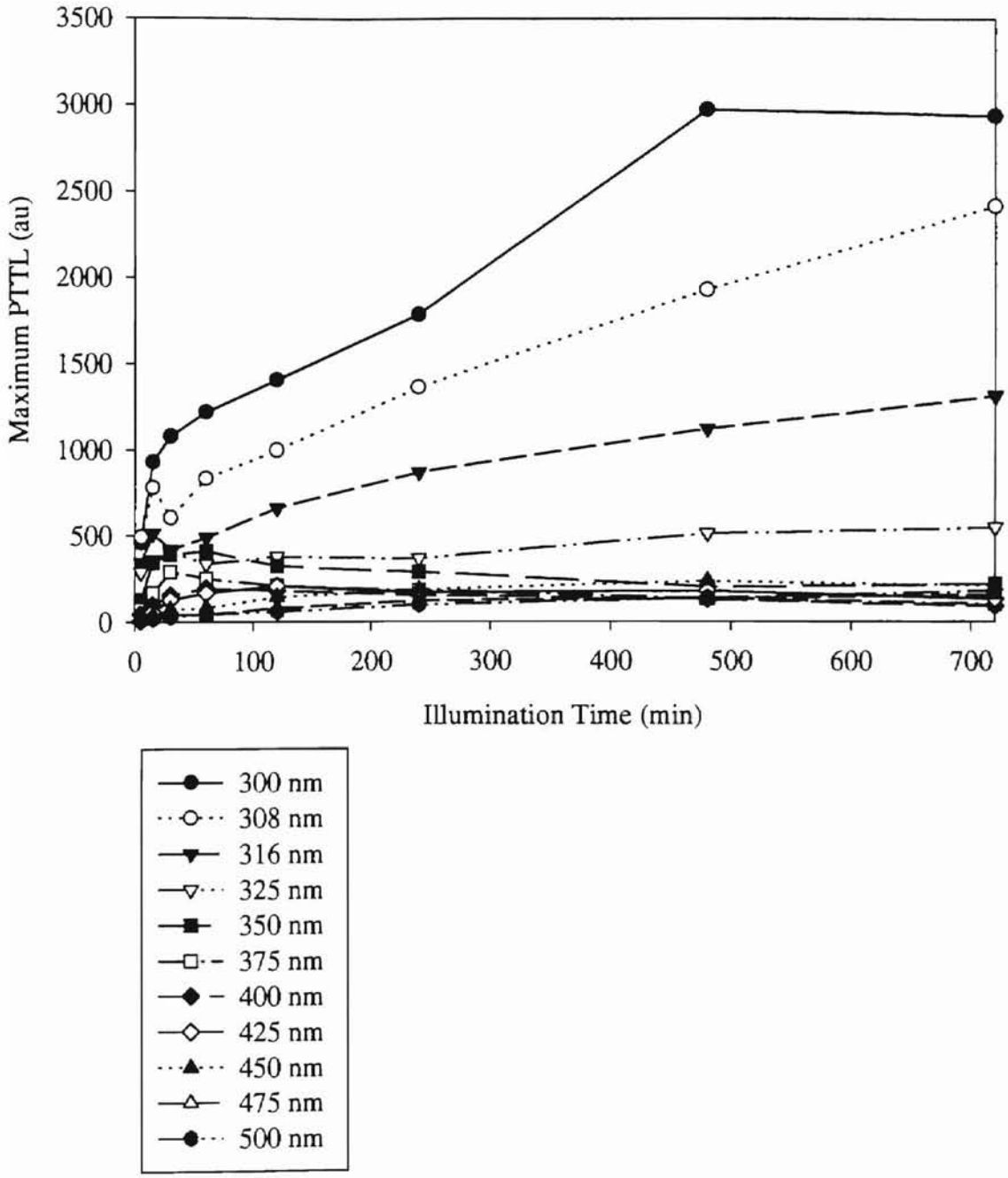

Figure 4.17: Premium-Q quartz maximum PTTL time response of the 270 K peak. Data is after illumination with light of the wavelength shown.

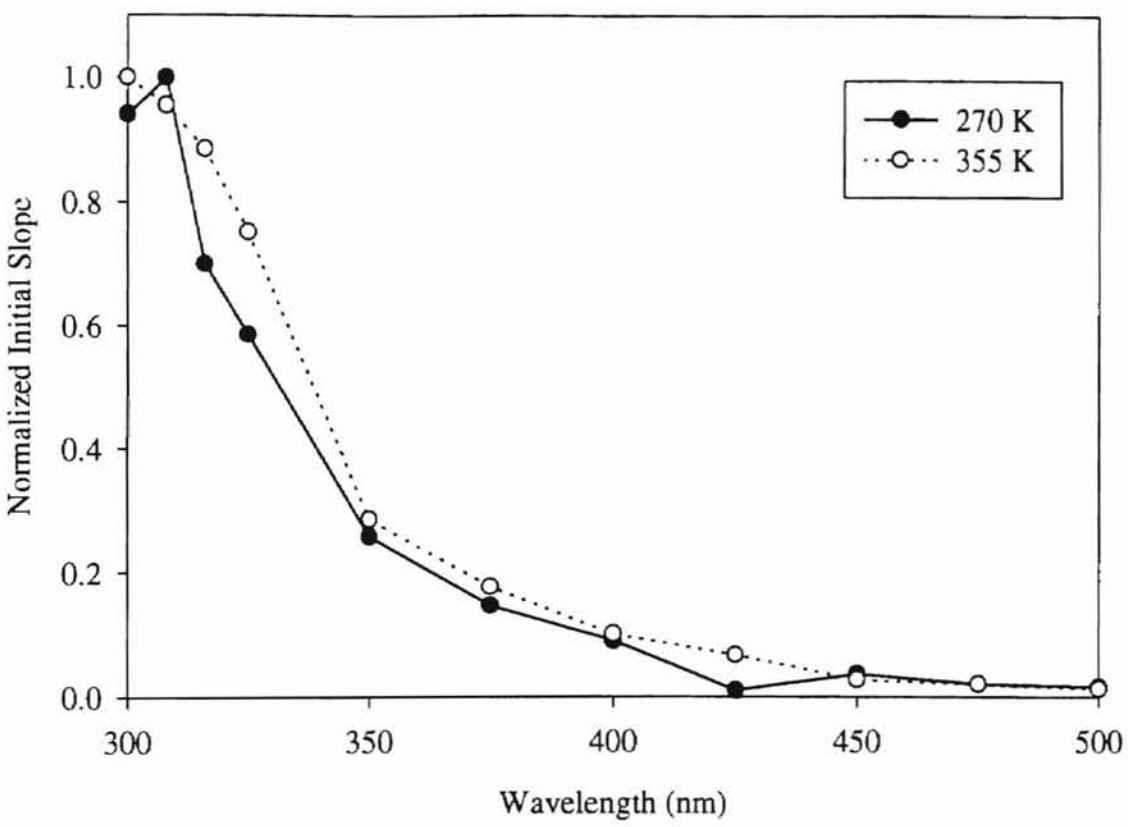

Figure 4.18: The initial slope of the maximum PTTL time response curves (figure 4.14) for Premium-Q quartz is plotted against the wavelength of the illumination light. Each curve represents a different PTTL peak.

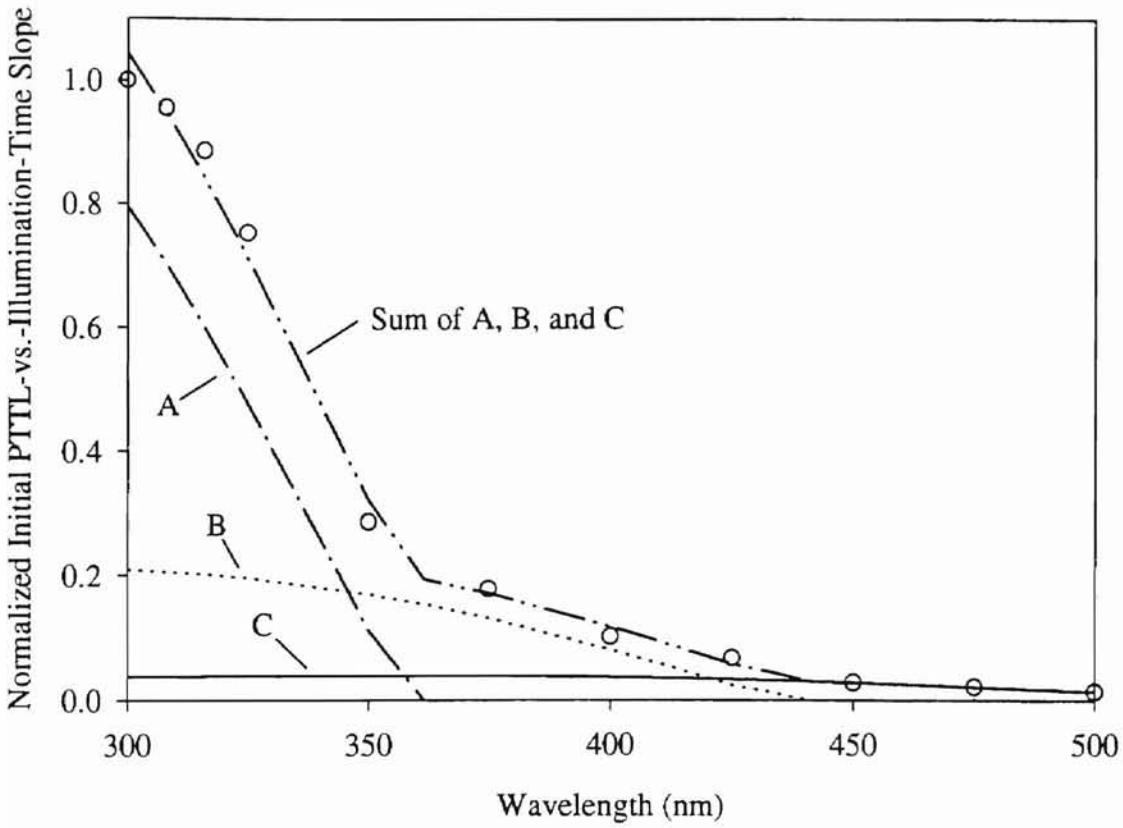

Figure 4.19: The initial slope data for the 355 K peak of figure 4.18 is shown (open circles) along with the numeric fit of equation 4.1. The three components of equation 4.1 are also shown (curves A, B, and C).

The wavelength dependence of the PTTL was determined by the initial slope method discussed above. The results are shown in figure 4.18. Again, there appears to be at least two and possibly three source traps being optically emptied over the wavelength range of 300 - 500 nm. The data were fit using equation 4.1. The fit is shown in figure 4.19. There is again good agreement between the fit and the data supporting further the claim that three source traps are present in this wavelength range. The optical ionization energies found were 2.27 eV, 2.81 eV, and 3.43 eV.

Summary and Conclusions of Chapter IV

Experimental results of PTTL response for both Arkansas natural quartz and Premium-Q synthetic quartz have been presented. These results show a varied behavior among different types of quartz and even between different traps present in the same quartz.

It was found that the PTTL signal does not decay to zero even after long bleaching times. This implies that the reduction of PTTL at long illumination times can not be caused by simultaneous excitation of electrons out of the traps responsible for the PTTL production. This supports the theory of McKeever (1991) that the reduction is caused by a loss of holes in the luminescent recombination centers during illumination.

A new method of analyzing experimental PTTL data was introduced. By plotting the initial slope of the PTTL illumination time response curves versus stimulation wavelength one can extract the shape of the wavelength dependence of the PTTL signal.

The wavelength response determined in this manner compares well with previously published data for bleaching of TL from quartz samples.

CHAPTER V

CONCLUSIONS AND FUTURE WORK

Summary and Conclusions

The analytical results presented in chapter II can be used to predict approximately the time response of the PTTL signal. Numerical solution of the differential equations provides what is considered to be an exact solution. PTTL is a complex process and can be simplified by making assumptions about the behavior of the models discussed. Each level of assumption causes the solutions obtained to deviate further from the exact numerical solution, but at the same time become more helpful in PTTL prediction.

Several models were solved numerically in chapter III. The most simple model which is capable of describing the PTTL process proved to be too simple in that it did not produce results similar to those obtained experimentally. The addition of a non-luminescent recombination center greatly improved the simple model. Further addition of a second donor trap produced results similar to the experimental results. There still exists a discrepancy that can not be explained at this time concerning the maximum PTTL signal. The addition of a deep trap to the model had no effect on the PTTL. These results are consistent with the findings of McKeever (1991).

Two types of quartz were examined experimentally. The results show a wide variation in the behavior of different types of quartz and also in different traps within the same samples.

It was found that the PTTL does not decay to zero even after extremely long bleaching times. This implies that the reduction of PTTL at long illumination times can not be caused by simultaneous excitation of electrons out of the traps responsible for the PTTL production. This supports the theory of McKeever (1991) that the reduction is caused by a loss of holes in the luminescent recombination centers during illumination.

The wavelength response of PTTL was extracted from the experimental data by a new method proposed in chapter IV. In this method, the initial slope of the PTTL time response curves is plotted versus the wavelength of the stimulation light. This produces the shape of the wavelength response. Results obtained in this manner were consistent with experimental results on the bleaching of TL obtained in this work and by other authors.

Future Work

There is still much work to be done on quartz. Further modeling should be performed to account for the discrepancy between the current simulated data and the experimental data concerning the maximum PTTL. This may also require further experiments to be performed at different wavelengths and illumination times. A study of the effects of small variations in stimulation wavelength and photon flux in the near-UV range may help explain some of the differences seen. The experiments conducted for this thesis were completed to the highest degree of precision available with this experimental apparatus. A more precise measurement of photon flux and the ability to control the

photon flux without changing the range of stimulation wavelengths may remove the discrepancies.

OSL experiments could be conducted to investigate the behavior of quartz during the illumination. This may also shed some light on the theoretical models.

The final goal of future work should be to construct a model which can accurately predict TL, PTTL, and OSL emissions given the initial conditions of the sample and details of the experiment to be performed. This is a lofty goal and is probably not achievable in the near future.

REFERENCES

Aitken, M.J. (1985) *Thermoluminescence Dating*. (Academic Press, New York)

Aitken M.J. and Smith B.W. (1988) Optical dating: Recuperation after bleaching. *Quat. Sci. Rev.* **7**, 387 - 393.

Bailiff, I.K. (1976). Use of phototransfer for the anomalous fading of thermoluminescence. *Nature*, **264**, 531.

Becker, K. (1973). *Solid State Dosimetry*. (CRC Press, Cleveland).

Böer, K.W. (1990) *Survey of Semiconductors Physics*. (Van Nostrand Reinhold, New York).

Bøtter-Jensen, L., Poolton, N.R.J., Willumsen, F., and Christiansen, H. (1994) A compact design for the monochromatic OSL measurements in the wavelength range 380 - 1020 nm. *Radiat. Meas.* **23**, 519

Bøtter-Jensen, L., Agersnap Larsen, N., Mejdahl, V., Poolton, N.R.J., Morris, M.F., and McKeever, S.W.S. (1995) Luminescence sensitivity changes in quartz as a result of annealing. *Radiat. Meas.* **24**, 535

Boyle, R. (1663) *Register of the Roy. Soc.*, **1663**, 213

Chen, R. and McKeever, S.W.S. (1997) *Theory of Thermoluminescence and Related Phenomena.* in preparation (World Scientific Publishers, New York)

Daniels, F., Boyd, C.A., and Saunders, D.F. (1953) Thermoluminescence as a research tool. *Science* **117**, 343

Ditlefsen, C. and Huntley, D.J. (1994) Optical excitation of trapped charges in quartz, potassium feldspars and mixed silicates; the dependence on photon energy. *Radiat. Meas.* **20**, 67?

Duller, G.A.T. and Bøtter-Jensen, L. (1996) Comparison of optically stimulated luminescence signals from quartz using different stimulation wavelengths. *Radiat. Meas.* (in press)

Grogler, N., Houtermans, F.G., and Stauffer, H. (1960) Ueber die datierung von keramik und ziegel durch thermolumineszenz, *Helvetica Physica Acta* **33**, 595

Huntley, D.J., Godfrey-Smith, D.L., and Thewalt, M.L.W. (1985) Optical dating of sediments. *Nature* **313**, 105

Jain, V.K. (1984) Photostimulated thermoluminescence in *Thermoluminescence and Thermoluminescence Dosimetry, Vol. II*, ed. Horowitz, Y.S. (CRC Press, Boca Raton) 173

Kennedy, G.C. and Knopff, L. (1960) Dating by thermoluminescence. *Archaeology* **13**, 147

Markey, B.G., Colyott, L.E., and McKeever, S.W.S. (1995) Time resolved optically stimulated luminescence from alpha Al_2O_3-C. *Radiat. Meas.* **24**, 457

McKeever, S.W.S. (1985) *Thermoluminescence of Solids*. (Cambridge University Press, New York)

McKeever, S.W.S. (1991) Mechanisms of thermoluminescence production: some problems and a few answers? *Nucl. Tracks Radiat. Meas.* **18**, 5

McKeever, S.W.S. (1994) Models for optical bleaching of thermoluminescence in sediments. *Radiat. Meas.* **23**, 267

McKeever, S.W.S., Bøtter-Jensen, L., Agersnap Larsen, N., and Duller, G.A.T. (1996) Temperature dependence of OSL decay curves: experimental and theoretical aspects. *Radiat. Meas.* (in press)

Milanovich-Reichhalter, I. and Vana, N. (1990) Phototransferred thermoluminescence in quartz. *Radiat. Prot. Dosim.* **33**, 211

Milanovich-Reichhalter, I. and Vana, N. (1991) Phototransferred thermoluminescence in quartz annealed at 1000° C. *Nucl. Tracks Radiat. Meas.* **18**, 67

Morris, M.F. (1995) Studies of optical bleaching of TL and OSL in quartz. M.A. thesis, Oklahoma State University, Oklahoma

Morris, M.F. and McKeever, S.W.S. (1994) Optical bleaching studies of quartz. *Radiat. Meas.* **23**, 323

Pierson, J., Forman, S.L., Lepper, K., and Conley, G. (1994) A variable narrow bandpass optically stimulated luminescence system for quaternary geochronology. *Radiat. Meas.* **23**, 533

Spooner, N.A. (1987) The effect of light on the thermoluminescence of quartz. M.S. thesis, University of Adelaide, Australia

Spooner, N.A. (1994) On the optical dating signal from quartz. *Radiat. Meas.* **23**, 593

Spooner, N.A., Prescott, J.R., and Hutton, J.T. (1988) The effect of illumination wavelength on the bleaching of the thermoluminescence (TL) of quartz. *Quat. Sci. Rev.* **7**, 325

Stokes, S. (1991) Optical dating of young (modern) sediments using quartz: results from a selection of depositional environments. *Quat. Sci. Rev.* **11**, 153

VITA

Charles Scott Alexander

Candidate for the degree of

Master of Science

Thesis: THEORETICAL AND EXPERIMENTAL ASPECTS OF PHOTOTRANSFERRED THERMOLUMINESCENCE FROM NATURAL AND SYNTHETIC QUARTZ

Major Field: Physics

Biographical:

Personal Data: Born in Redlands, California, on June 17, 1971, the son of Charles R. and Nancy L. Alexander.

Education: Graduated from Redlands High School, Redlands, California in June 1989; received Bachelor of Science degree in Physics and Bachelor of Arts degree in Applied Mathematics from the University of California, San Diego, La Jolla, California in March, 1994. Completed the requirements for the Master of Science degree with a major in Physics, at Oklahoma State University, Stillwater, Oklahoma, in July, 1996.

Professional Membership: American Physical Society